

THESIS

## LIBRARY Michigan State University

This is to certify that the dissertation entitled

## INVESTIGATION OF METAL NANOPARTICLES ENCAPSULATED IN POLYELECTROLYTE MULTILAYERS FOR CATALYTIC AND ANTIBACTERIAL APPLICATIONS

presented by

#### SRIVIDHYA KIDAMBI

has been accepted towards fulfillment of the requirements for the

Ph.D.	degree in	Ch	emistry
	<b>7</b> . s	_	
Me	Major Bro	fessor's Signati	liro /
	(5) 18	(	ure
		Date	<u> </u>

MSU is an affirmative-action, equal-opportunity employer

PLACE IN RETURN BOX to remove this checkout from your record.

TO AVOID FINES return on or before date due.

MAY BE RECALLED with earlier due date if requested.

DATE DUE	DATE DUE	DATE DUE
2012		
OCT 1 5 2010		

6/07 p:/CIRC/DateDue.indd-p.1

# INVESTIGATION OF METAL NANOPARTICLES ENCAPSULATED IN POLYELECTROLYTE MULTILAYERS FOR CATALYTIC AND ANTIBACTERIAL APPLICATIONS

By

Srividhya Kidambi

## **A DISSERTATION**

Submitted to
Michigan State University
in partial fulfillment of the requirements
for the degree of

**DOCTOR OF PHILOSOPHY** 

Department of Chemistry

2007

## **ABSTRACT**

## INVESTIGATION OF METAL NANOPARTICLES ENCAPSULATED IN POLYELECTROLYTE MULTILAYERS FOR CATALYTIC AND ANTIBACTERIAL APPLICATIONS

By

#### SRIVIDHYA KIDAMBI

Metal nanoparticles are an interesting class of materials because they often exhibit properties different from those of the corresponding bulk metals. For example, bulk Au is not catalytically active, but recent studies show that Au nanoparticles can serve as catalysts for oxidation and hydrogenation reactions. Without a suitable support, however, metal particles aggregate, reducing surface area and eventually affecting the particle properties. To overcome this problem, this research employs the layer-by-layer (LbL) assembly technique, which was introduced by Decher in 1991, as a convenient method to prevent the aggregation of nanoparticles and immobilize them on solid supports. While the multilayers help in stabilizing the nanoparticles, they also aid in retaining important properties of Pd (catalytic) and silver (antibacterial) nanoparticles.

Catalytic Pd nanoparticles in multilayer polyelectrolyte films can be easily prepared by alternating depositions of poly(acrylic acid) (PAA) and a polyethylenimine (PEI)-Pd(II) complex on alumina, and subsequent reduction of the Pd(II) by NaBH<sub>4</sub>. The polyelectrolytes limit aggregation of the particles and impart catalytic selectivity in the hydrogenation of  $\alpha$ -substituted unsaturated alcohols by restricting access to catalytic sites. Hydrogenation of allyl alcohol by encapsulated Pd(0) nanoparticles can occur as much as 24-fold faster than hydrogenation of 3-methyl-1-penten-3-ol. In a related

system, alternating adsorption of PdCl<sub>4</sub><sup>2</sup> and polyethylenimine (PEI), followed by reduction of Pd(II), yields catalysts with a higher activity than found in [PAA/PEI-Pd(0)]<sub>n</sub>PAA films due to greater accessibility of the Pd nanocatalysts. In the [PAA/PEI-Pd(0)]<sub>n</sub>PAA system, turnover frequency decreases with the number of layers deposited, suggesting that the outer layer of the film is primarily responsible for catalysis. In contrast, turnover frequency increases with the number of deposited layers for reduced [PdCl<sub>4</sub><sup>2</sup>/PEI]<sub>n</sub> films.

We also report work examining the antibacterial properties of Ag nanoparticle-containing multilayer polyelectrolyte films deposited on polyethersulfone ultrafiltration membranes. Rubner and others suggested that the mechanism of antibacterial action by Ag nanoparticles in polyelectrolyte films presumably involves oxidation of nanoparticles and slow release of Ag<sup>+</sup>. In principle, this should lead to sustained antibacterial efficacy of membranes containing Ag nanoparticles compared to membranes containing Ag<sup>+</sup> ions. Studies of silver leaching confirm that the rate of leaching of silver in Ag<sup>+</sup>-containing films is nearly an order of magnitude greater than that in Ag<sup>0</sup>-nanoparticle containing systems, confirming that the use of Ag nanoparticles rather than ions could enhance the longevity of an antibacterial coating. Filtration of bacteria-containing suspensions through modified membranes indicates that the flux decline associated with bacterial fouling in silver-containing films is lower than that in membranes without any silver coating, but it is difficult to distinguish between Ag<sup>+</sup> and Ag<sup>0</sup>-containing films in short-term fouling studies.

TO MY FAMILY

## **ACKNOWLEDGMENTS**

I would like to express my deepest appreciation to my advisor Dr. Merlin Bruening, for his guidance and invaluable assistance, without which this thesis would not have been possible. I appreciate the freedom and encouragement Merlin gave me and his tolerance of my independent streak in pursuing the research both during times when the research was in its difficult stages and when it was sailing smoothly. I have learnt several things from him about research, and writing and presenting the research performed. He has influenced me in many ways than what I actually realize.

I would also like to thank the members of my Ph.D. committee, Dr. Gary Blanchard, Dr. Babak Borhan, and Dr. Ilsoon Lee. I would have to thank Babak in particular for letting me use his resources for the antibacterial project. I would like to convey my heartfelt thanks to my collaborator for the antibacterial project, Dr. Vladimir Tarabara.

I am also thankful to my group members whom I learned a lot from. I would like to thank both the current and past members for making my Ph.D. a pleasant experience. Thanks to Jamie, Lu, Maneesha, Lei, Jinhua Dai, Fei, David, Parul, Somnath, Jin, Matt, Dan, Christin, Brian, Malai, and Xiaoyun. In particular, I thank Lei, Jamie, Maneesha and Lu for all the fun time we had together.

Particularly due to this thesis's interdisciplinary nature, I also got benefited greatly from collaborative environment. I need to pay gratitude to our collaborators in France and Ukraine. The most notable person includes Vita from Kiev, who helped me in some of the antibacterial experiments. Also, thanks to Lu, Wen, and Julian for the memorable experience we had in Europe, most of them being nice.

Thanks to Per Askeland for helping me with XPS experiments. Also, I highly appreciate the help offered by Ewa and Alicia in SEM and TEM experiments respectively. Special mention goes to Kathy for all her help with the instruments in the A/P labs.

It would be an understatement to say that my stay in MSU has been memorable experience because of my friends. I would particularly like to thank Priya and Thara, for all the wonderful discussions we had about pretty much everything under the sun, and many other things small and large, that contributed to my Ph.D., often in unpredictable ways.

And to my family I owe the maximum gratitude, for years of their constant support, patience and understanding. They provided me with the drive to finish with their generous encouragement. To all of them, Amma, Appa, Srikanth (Annathey), Manni, Srivats, Patti, Mamas, Mamis, all the kuttis and many many others I owe my heartfelt thanks for always being there for me.

## **TABLE OF CONTENTS**

LIST OI	F TABLES	<b>(</b>
LIST OI	F SCHEMESx	(i
LIST OI	F FIGURESx	ii
LIST OI	F ACRONYMSx	(V
Chapte	er 1: Background Information	1
1.1.	Introduction	1
1.2.	History and Development of Layer by Layer Assembly	
1.3.	Incorporation of Nanoparticles in PEM Films to Form Composite Material	
1.4.	Motivation and Research Goals	
1.4.1.	Application of Encapsulated Nanoparticles in Selective Catalysis	
1.4.2.	Application of Encapsulated Nanoparticles as Antibacterial Coatings o	n
	Membranes	9
1.5.	Outline of the Thesis	
1.6.	References	.13
	r 2: Selective Hydrogenation By Pd Nanoparticles Embedded In crylic Acid)/Polyethyleneimine Multilayers2	
2.1.	Experimental Section.	
2.2.	Materials	
2.2.2.	Preparation of Pd Nanoparticles Encapsulated in PAA/PEI multilayer	
2.2.2.	filmsfilms	
2.2.3.	Characterization of Pd Nanoparticles.	
2.2.4.	Hydrogenation Reactions	
2.2.5.	Determination of the Amount of Pd in Catalysts	
2.2.6.	Determination of Transport Rates by Diffusion Dialysis	
2.2.0.	Results and Discussion	
2.3.1.	Film Deposition	
2.3.2.	Film Characterization.	
2.3.3.	Selective Catalysis of Hydrogenation	
2.3.4.	Mechanism of Selective Hydrogenation	

2.4.	Conclusions	38
2.5.	References	
	r 3: Pd Nanoparticles Encapsulated in Reduced [PdCl <sub>4</sub> <sup>2-</sup> /PEI] <sub>n</sub> Films: Active Catalysts for Selective Hydrogenation	43
3.1.	Introduction	42
3.2.	Experimental Section.	
3.2.1.	Materials	
3.2.2.	Preparation of Pd Nanoparticles Encapsulated in PAA/PEI multilaye	er
3.2.3.	Characterization of Pd Nanoparticles	
3.2.4.	Transport Studies.	
3.2.5.	Hydrogenation Reactions	45
3.2.6	Determination of the Amount of Pd in Catalysts and Deposition	
2.2	Solutions	
3.3.	Results and Discussion.	
3.3.1.	Film Deposition	
3.3.2.	Film Characterization	
3.3.3.	Catalysis of Hydrogenation	
	3.1. Reaction Kinetics	
3.3	.3.2. Catalytic Activity of Reduced [PdCl <sub>4</sub> <sup>2</sup> /PEI] <sub>n</sub> as a Function of the	
2.2	Substrate and Film Composition	
3.3	.3.3. Catalytic Activity of Reduced [PAA/PEI-Pd(0)] <sub>n</sub> PAA as a Function	
	of the Substrate and Film Composition.	
3.3.4.	,	
3.3.5.		
3.4.	Conclusions	
3.5.	Reference	66
	r 4: Multilayer Polyelectrolyte Films Containing Silver nanoparticles A	
	Introduction	
4.1. 4.2.	Experimental Section.	
4.2.1.	Materials	
4.2.2.	Film Deposition on polyethersulfone membranes	
4.2.3.	Film Characterization.	
4.2.3.	Leaching of Ag from multilayer films on polymer supports	
4.2.5.		
4.2.5.	Bacteria and culture conditions.	
	Examination of the Inhibition of Bacterial Growth by Scanning Electroscopy	
4.2.7.	Examination of the Inhibition of Bacterial Growth by Optical Microscopy	
4.2.8.	Long-term Dead-end Filtration of Bacterial Suspensions	
4.3.	Results and Discussion.	
4.3.1.	Layer-by-layer growth of polyelectrolyte using reflectance FT-IR	76
4.3.2.	Film Characterization.	77

4.3.3.	Evaluation of Anti-microbial properties using Microscopy	78
4.3.4.	Leaching of Ag from multilayer films on polymer supports	
4.3.5.	Changes in Flux during Filtration of Bacterial Suspension	
4.4.	Conclusions	
4.5.	References	92
Chapte	r 5: Conclusions and Future Work	96
5.1.	Incorporation of metal nanoparticles in polyelectrolyte multilayer films	for
	selective catalysis	96
5.2.	Application of Ag nanoparticles in polyelectrolyte multilayer films as	
	antibacterial coatings	97
5.3.	Future Work: Selective Catalysis	97
5.3.1.	Selective hydrogenation of dienes	
5.3.2.	Synergistic effect using bimetallics	
5.4.	Future Work: Antibacterial Coatings	
5.5.	Summary Statement	
5.6.	References	

## LIST OF TABLES

Table 2.1	Turnover Frequencies (TOFs) for hydrogenation of structurally related unsaturated alcohols by several Pd catalysts33
Table 3.1	TOFs (moles hydrogenated per mol Pd per h) for hydrogenation of allylic alcohols using several catalysts
Table 3.2	Hydrogenation TOFs for catalysts containing [PAA/PEI-Pd(0)] <sub>n</sub> PAA films on alumina with several values of n
Table 3.3	Hydrogenation TOFs for reduced [PdCl <sub>4</sub> <sup>-2</sup> /PEI] <sub>3</sub> films on alumina63

## **LIST OF SCHEMES**

Scheme 1.1	Schematic diagram of the "Dip and Rinse" procedure used for the layer- by-layer deposition of a bilayer of a polyelectrolyte multilayer film5
Scheme 2.1	Formation of Nanoparticles in PEMs26
Scheme 3.1	Formation of Pd nanoparticles in reduced [PdCl <sub>4</sub> <sup>2</sup> /PEI] <sub>n</sub> films44
Scheme 4.1	Preparation of Ag nanoparticles embedded in polyelectrolyte multilayer films
Scheme 4.2	Initial assay of bacterial growth74

## **LIST OF FIGURES**

Figure 1.1.	Number of publication concerning nanoparticles listed in a SciFinder
	Scholar (American Chemical Society search engine) search
Figure 1.2	Worldwide market of nanoparticles in 2000 and 2005 for various applications as reported by Business Communications Company, Inc. in 2001
Figure 2.1	Home-built diffusion dialysis set-up for transport experiments (Figure courtesy of Dr. Jinhua Dai)29
Figure 2.2	UV-Vis absorption spectra of [PEI-Pd(II)/PAA] <sub>n</sub> PEI-Pd(II) films on quartz substrates with $n = 0, 1, 2,$ and 3 (from lower to upper curves)30
Figure 2.3	TEM image of [PAA/PEI-Pd(0)]PAA on a carbon-coated copper grid31
Figure 2.4	Percent of substrate hydrogenated vs reaction time for allyl alcohol (squares), 1-penten-3-ol (triangles), and 3-methyl-1-penten-3-ol (diamonds) using 3.5-bilayer PAA/PEI-Pd(0)-coated alumina as a catalyst. Percent hydrogenation was obtained from the integration of product and reactant peaks in gas chromatograms
Figure 2.5	Receiveing phase concentration as a function of time during diffusive transport of substrates through 0.02 µm-alumina membrane coated with (PAA/PEI) <sub>7</sub> film. The substrates were allyl alcohol (squares), 1-penten-3-ol (triangles), and 3-methyl-1-penten-3-ol (diamonds). The source phase contained 20 mM of each substrate in water while the receiving phase initially contained deionized water. Receiving phase concentrations were determined from the integration of substrate peaks in gas chromatograms.
Figure 3.1	UV-Visible absorption spectra of [PEI/PdCl <sub>4</sub> <sup>2-</sup> ] <sub>n</sub> films on a quartz substrate with $n = 1$ to 7 (from lower to upper curves), (a). (b) shows the absorbance at $\lambda_{\text{max}}$ (220 nm) as a function of number of bilayers50
Figure 3.2	(A) Micromoles of Pd (determined by atomic emission spectroscopy) per g of catalyst for several values of n in [PdCl <sub>4</sub> <sup>2</sup> -/PEI] <sub>n</sub> films deposited on alumina. (Analysis was performed after reduction of the Pd(II) with NaBH <sub>4</sub> as described in the text.) (B) The corresponding plot for

F

	[PAA/PEI-Pd(0)] <sub>n</sub> PAA films on alumina52
Figure 3.3	(a) TEM image of a [PdCl <sub>4</sub> <sup>2-</sup> /PEI] <sub>3</sub> film deposited on a carbon-coated copper grid and reduced with NaBH <sub>4</sub> and (b) the histogram of particle sizes obtained from the above TEM image
Figure 3.4	(a) XPS spectra of a [PAA/PEI-Pd] <sub>3</sub> PAA film on alumina before (bottom) and after (top) reduction with NaBH <sub>4</sub> . (b) Corresponding spectra of [PdCl <sub>4</sub> <sup>2</sup> -/PEI] <sub>3</sub> films on alumina
Figure 3.5	Amount of allyl alcohol hydrogenated vs reaction time for 200-Ml solutions initially containing 20 mmol (diamonds), 2 mmol (triangles), and 0.2 mmol (squares) of allyl alcohol. The catalyst was 250 mg of alumina coated with a reduced [PdCl <sub>4</sub> <sup>2</sup> -/PEI] <sub>3</sub> film
Figure 4.1	Reflectance FTIR spectra of [PEI/PSS] <sub>n</sub> films on Au with n varying from 1-5
Figure 4.2	TEM image of a (PSS/PEI-Ag <sup>0</sup> ) <sub>4</sub> /PSS film on a carbon-coated copper grid
Figure 4.3	SEM images of PES membrane surfaces that were coated with (PSS/PEI) <sub>4</sub> /PSS (A), (PSS/PEI-Ag <sup>+</sup> ) <sub>4</sub> /PSS (B), or (PSS/PEI-Ag <sup>0</sup> ) <sub>4</sub> /PSS (C) and subsequently treated by filtration of 3 mL of bacteria (10 <sup>7</sup> cells/mL), incubation in LB broth for 18 h, and fixation of bacteria with a formaldehyde/glutaraldehyde mixture80
Figure 4.4	Optical micrographs of PES membranes that were uncoated (1-control), or coated with (PSS/PEI) <sub>4</sub> /PSS (2), (PSS/PEI-Ag <sup>+</sup> ) <sub>4</sub> /PSS (3), or (PSS/PEI-Ag <sup>0</sup> ) <sub>4</sub> /PSS (4), and subsequently used to filter 3 mL of bacterial suspensions prior to incubation in Endo medium for 10 days. (Figure courtesy of Dr. Viktoriya Konovalova)
Figure 4.5	Amount of silver leached from PES membranes coated with (PSS/PEI)₄/PSS (♠), (PSS/PEI-Ag <sup>+</sup> )₄/PSS (♠), and (PSS/PEI-Ag <sup>0</sup> )₄/PSS (■) during immersion in LB broth without stirring. Broth samples were analyzed by AAS
Figure 4.6	Temporal flux profiles during filtration of deionized water or bacterial suspensions (10 <sup>8</sup> cells/mL of deionized water) through PES membranes coated with (PSS/PEI) <sub>4</sub> /PSS (a), (PSS/PEI-Ag <sup>+</sup> ) <sub>4</sub> /PSS (b), and (PSS/PEI-Ag <sup>0</sup> ) <sub>4</sub> /PSS (c). The transmembrane pressure was 4.8 bar
Figure 4.7	SEM images of PES membranes that were coated with (PSS/PEI) <sub>4</sub> /PSS (a), (PSS/PEI-Ag <sup>+</sup> ) <sub>4</sub> /PSS (b), or (PSS/PEI-Ag <sup>0</sup> ) <sub>4</sub> /PSS (c) and

	subsequently used to filter a bacterial suspension (10 <sup>8</sup> cells/mL) for 15-16 h. Bacteria were fixed with glutaraldehyde prior to imaging87
Figure 4.8	Temporal Flux (a) and normalized temporal flux (b) profiles during bacteria filtration with PES membranes modified with different coatings at a constant pressure of 4.8 bar. (PSS/PEI) <sub>4</sub> /PSS- red; (PSS/PEI-Ag <sup>+</sup> ) <sub>4</sub> /PSS-green, and (PSS/PEI-Ag <sup>0</sup> ) <sub>4</sub> /PSS-blue. The feed filtration solutions initially contained 10 <sup>8</sup> cells/mL
Figure 4.9	Temporal Flux (a) and normalized temporal flux (b) profiles during filtration of bacterial solutions through PES membranes coated with (PSS/PEI) <sub>4</sub> /PSS- red; (PSS/PEI-Ag <sup>+</sup> ) <sub>4</sub> /PSS-green, and (PSS/PEI-Ag <sup>0</sup> ) <sub>4</sub> /PSS-blue. The feed filtration solutions initially contained 10 <sup>8</sup> cells/mL, and filtration pressures were selected to give similar initial flux values (see text)

## LIST OF ACRONYMS

LbL: Layer-by-Layer

**PEI:** Poly(ethyleneimine)

**PSS:** Poly(styrenesulfonate)

PAA: Poly(acrylicacid)

**PES:** Polyethersulfone

**PEM:** Polyelectrolyte Multilayers

**XPS:** X-ray Photoelectron Spectroscopy

**PEM:** Polyelectrolyte Multilayer

TEM: Transmission Electron Microscopy

**SEM:** Scanning Electron Microscopy

UV-Vis: UV-Visible

AAS: Atomic Absorption Spectroscopy

E.Coli: Escherichia coli

FTIR: Fourier Transform Infrared Spectroscopy

## **Chapter 1: Background Information**

#### 1.1. Introduction

This thesis aims to illustrate a simple procedure for preparing metal nanoparticles incorporated in polyelectrolyte multilayer films, which has a tremendous potential for creating selective catalysts and antibacterial coatings. The widespread realization that metal nanoparticles have a remarkable potential in a variety of applications is evident from the exponential increase in the number of publications related to nanoparticles in the last several years (Figure 1.1). On the other hand, the commercial use of nanoparticles is not as extensive as the number of publications in this area might suggest (Figure 1.2), with sales only approximately doubling from 2000-2005. The relatively small industrial market for nanoparticles may be attributed to the difficulty not only in making the particles in nano-scale dimensions, but also in retaining them as nanoparticles after their formation. This is because nanoparticles have a general tendency to aggregate, thus forming a less desirable agglomerated morphology. This issue of aggregation could be a serious challenge for various applications such as catalysis, where the size of the nanoparticles plays an important role in deciding their properties.<sup>2</sup> In this chapter, I introduce the general procedure of layer by layer assembly which can be employed to address this challenge of aggregation of nanoparticles. Also, I discuss some of the other techniques that have been employed to prepare and stabilize nanoparticles, particularly for catalytic applications. Subsequently, a brief background of the use of metal nanoparticles in the area of antibacterial coatings is discussed. Finally I present the outline of the dissertation.

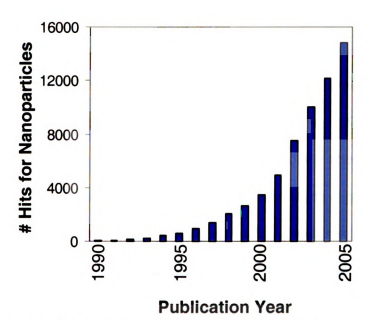


**Figure 1.1.** Number of publication concerning nanoparticles listed in a SciFinder Scholar (American Chemical Society search engine) search. "Images in this dissertation are presented in color"

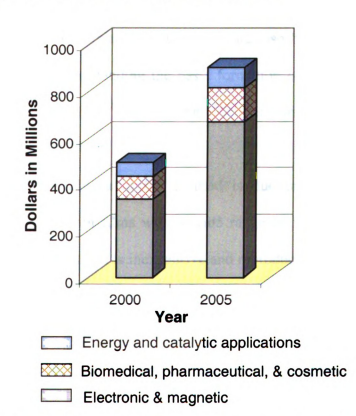


**Figure 1.2.** Worldwide market of nanoparticles in 2000 and 2005 for various applications as reported by Business Communications Company, Inc. in 2001

C

co

РC

the

۶ü

āno

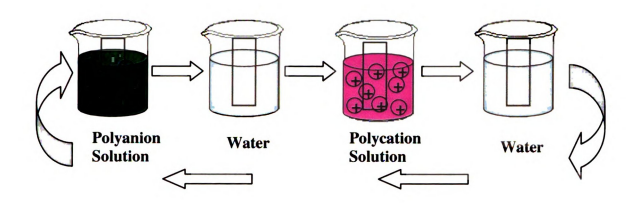
#### 1.2. History and Development of Layer by Layer Assembly

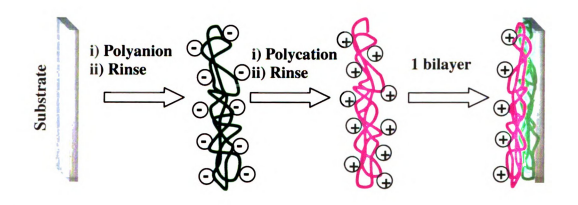
In the early 1990s, an interesting technique for building ultrathin polymer films, layer by layer (LbL) assembly of polyelectrolytes, was developed by Decher and coworkers.<sup>3-5</sup> This method has become widely used over the last 15 years because it of its simplicity and versatility.<sup>6</sup> LbL assembly simply involves alternate adsorption of polycations (positively charged polymers) and polyanions (negatively charged polymers) on literally any substrate. Such films are being applied in a wide range of research areas from sensors and electronics<sup>7-9</sup> to tissue engineering<sup>10, 11</sup> and biotechnology<sup>12, 13</sup>. This explosion in interest can be attributed to the flexibility achieved by using different polyelectrolytes for the formation of multilayers on any substrate for many applications. Not only has the application aspect of these polyelectrolyte multilayers (PEMs) aroused widespread interest, but theoretical aspects of LbL are also being investigated. Many studies have focused on understanding the basic formation of PEMs and the effect of various parameters such as pH<sup>14-17</sup>, ionic strength<sup>18-21</sup>, temperature<sup>22, 23</sup>, and solvent<sup>24, 25</sup> on film growth.

The popularity of LbL assembly method is due primarily to its ability to controllably form polymer thin films with a wide range of functional groups using a convenient deposition process that is inexpensive and reproducible (Scheme 1.1). In this method, a charged substrate is immersed into a solution of oppositely charged polyelectrolyte. A layer of a polyion adsorbs due to electrostatic interactions between the substrate and the polyelectrolyte. This process is driven by the increase in entropy due to the displacement of counter-ions from the surface of the deposited polyelectrolyte chain and from the substrate.<sup>26</sup> This step is followed by rinsing with water, which removes any

excess of the unadsorbed polyelectrolyte solution, and subsequent immersion into an oppositely charged polyelectrolyte results in another layer on the substrate. This sequence of steps yields a "bilayer" of polyelectrolyte film, and the procedure can be repeated as many times as necessary depending on the application, to form PEMs. The technique, which was initially started with simple polyamines and polysulfonates, has now branched out to the incorporation of literally any charged species including electroactive polymers, <sup>27, 28</sup> quantum dots, <sup>29-31</sup> DNA, <sup>32-34</sup> charged viruses, <sup>35, 36</sup> inorganic sheets, <sup>27, 37, 38</sup> and a wide variety of proteins, <sup>39-42</sup> enzymes, <sup>43-47</sup> and other biosystems. <sup>48-50</sup> One of the most advantageous and interesting aspects of the LbL-technique is that active macromolecules can be introduced in the polyelectrolyte multilayer films without significantly altering their electrical, chemical or biological properties.

Although layer-by-layer assembly of polymeric electrolytes began in the 1990's, the precedent for such assembly was established in 1966 in the layer-by-layer assembly of oppositely charged colloidal particles by Iler.<sup>51</sup> With either colloids or polymeric electrolytes, one advantage of this technique is that electrostatic attractions between opposite charges are flexible and yet they tightly hold the film together. Another advantage over the classical Langmuir-Blodgett technique is that adsorption processes are independent of substrate size and topology. Also in contrast to the Langmuir-Blodgett technique, one can work with water-soluble molecules in LbL assembly, which is a prerequisite for deposition of many functional macromolecules.





**Scheme 1.1.** Schematic diagram of the "Dip and Rinse" procedure used for the layer-by-layer deposition of a bilayer of a polyelectrolyte multilayer film.

## 1.3. Incorporation of Nanoparticles in PEM Films to Form Composite Materials

Nanotechnology is expected to be the basis of many of the main scientific and industrial innovations of the 21<sup>st</sup> century, and there is tremendous growth in the research and development of this field throughout the world.<sup>52</sup> A major outcome of this global interest is the development of new materials in the nanometer scale, including nanoparticles. Metal nanoparticles are an interesting class of materials because they often exhibit properties different from those of the corresponding bulk metals.<sup>53-58</sup> For example, bulk Au is not catalytically active, but recent studies show that Au nanoparticles can serve as catalysts for oxidation and hydrogenation reactions.<sup>2, 59</sup> Additionally, nanoparticle properties can be tuned by varying their sizes<sup>2, 57, 59</sup> and environments.<sup>60</sup> Because of these unique characteristics, metal nanoparticles are being intensively studied for applications in catalysis,<sup>57, 61</sup> optoelectronics,<sup>62</sup> preservatives,<sup>63</sup> and sensing<sup>64</sup>.

Without a suitable support, however, metal particles aggregate, reducing surface area and eventually affecting the properties of the particles. To overcome this problem, metallic nanoparticles have been immobilized on solid supports, e.g., carbon, 65 metal oxides, 66 and zeolites, 67, 68 or stabilized by capping ligands that range from small organic molecules to large polymers 69-72. Encapsulation by polymers is advantageous because in addition to stabilizing and protecting the particles, polymers offer unique possibilities for modifying both the environment around catalytic sites and access to these sites. In this thesis, we present the application of metal nanoparticles encapsulated in polyelectrolyte multilayer films for selective catalysis and as antibacterial coatings.

#### 1.4. Motivation and Research Goals

## 1.4.1. Application of Encapsulated Nanoparticles in Selective Catalysis

Catalysis provides a natural application for nanoparticles because their large surface area-to-volume ratio allows effective utilization of expensive metals, and research in this area has increased dramatically in the last several years. Catalysis by nanoparticles has been termed "semi-heterogeneous catalysis" because it represents a transition between molecular, homogeneous catalysts and less controlled heterogeneous materials. Using nanoparticles, there have been improvements not only in the efficiency and selectivity of reactions, but also in the recovery and recyclability of the catalytic materials. Typically nanocatalysts are prepared from a metal salt, a reducing agent, and a stabilizer and are supported on oxides, charcoal, or zeolites. There are a wide range of stabilizers that have been explored to prevent the aggregation of nanoparticles such as metal-binding ligands, surfactants, dendrimers and polymers.

The use of ligands for stabilizing metal nanoparticles has been of great importance since they can also be employed to tune the properties of the catalytic materials. This helps in controlling and optimizing the catalytic efficiency to obtain the desired properties such as high yield and selectivity. One group of commonly used ligand stabilizers are organothiols. Pd nanoparticles stabilized by dodecanethiol can be used as recyclable catalysts in the Suzuki reaction of chloroarenes with phenylboronic acid at ambient temperature. Enantioselective reactions have also been successfully carried out with metal nanoparticles to achieve high ee values. One of the earliest asymmetric reaction catalyzed by metal nanoparticles used Rh nanoparticles during the hydrogenation of 2-methylanisole o-cresol trimethylsilyl ether, where Rh nanoparticles

with chiral amines as ligands induced enantioselectivity.<sup>78</sup> Pt orPd nanoparticles capped with cinchonidine ligands were employed during the hydrogenation of ethyl pyruvate with an ee of upto 98%.<sup>79</sup> Also, enantioselective allylic alkylation reactions were reported with 97% ee using catalysis by Pd nanoparticles stabilized in the presence of chiral xylofuranide diphosphite.<sup>81</sup>

Surfactants have also been widely employed to stabilize nanoparticles. Recently, Pd nanoparticles stabilized by N,N-dimethyl-N-cetyl-N-(2-hydroxyethyl)ammonium chloride salt have been investigated for catalytic hydrogenation and dehalogenation of various halogenoarenes. Also, cetyltrimethylammonium bromide was reported to promote and stabilize the formation of metallic Cu nanoparticles on several metal oxides, which were employed for the selective dehydrogenation of methanol to produce formaldehyde and hydrogen with 100% H<sub>2</sub> selectivity. 83

Recently, there has been a lot of interest in using polymers as innovative stabilizers. Polymers stabilize metal nanoparticles using their steric bulk framework, which prevents nanoparticle aggregation. Moreover, polymers can also weakly bind to the nanoparticle surface through heteroatoms that can impart certain desired properties. Poly(N-vinyl-2-pyrrolidone) (PVP), for example, has been commonly used for nanoparticle stabilization and catalysis. PVP-stabilized Pt, Pd, and Rh nanoparticles that are synthesized by the reduction of the corresponding metal halide in refluxing ethanol and immobilized in an ionic liquid are very efficient olefin and benzene hydrogenation catalysts at 40°C, and these catalysts can be recycled without loss of activity. Also, palladium and bimetallic (PdAu, PdPt, and PdZn) nanoparticles were stabilized in block

copolymer micelles derived from polystyrene-block-poly-4-vinylpyridine (PS-b-P4VP) and studied in selective hydrogenation of dehydrolinalool.<sup>85</sup>

Another commonly used polymer type that that has been recently explored extensively for nanoparticle stabilization is dendrimers. Richard Crooks has pioneered the use of metal nanoparticles encapsulated in dendrimer systems. There are several advantages in using a dendrimer as the stabilizing agent. (1) the dendrimer templates possess uniform composition and structure, and therefore they yield well-defined nanoparticle; (2) the nanoparticles are stabilized by encapsulation within the dendrimer, thereby preventing particle agglomeration; (3) the encapsulated nanoparticles in dendrimer systems are catalytically active; (4) the dendrimer branches can be used to selectively control access of small molecules to the encapsulated nanoparticles; (5) the functionality on the dendrimer can be tailored to control solubility of the hybrid nanocomposite. This work shows that nanoparticles in PEMs show catalytic selectivities that are equivalent to those in dendrimers.

## 1.4.2. Application of Encapsulated Nanoparticles as Antibacterial Coatings on Membranes

Antimicrobial surface modifications help in preventing growth of detrimental microorganisms, which is a highly desired goal. The potential use of antimicrobial surface coatings appears in fields ranging from medicine, <sup>87-89</sup> where medical device infection is associated with significant healthcare costs, to the construction, <sup>90, 91</sup> textile, <sup>92</sup> and food industries <sup>93, 94</sup>. Microbial adhesion to surfaces is usually followed by cell growth, thus resulting in the formation of a complex biofilm matrix capable of protecting

b

C

at

eŋ

the of s

Will

the underlying microbes from antibiotics and host defense mechanisms. <sup>95, 96</sup> In the case of biomedical devices such as catheters, prosthetics, and implants, surface microbial contamination can result in critical infection and device failure. <sup>97</sup> Hence, there is a significant interest in the development of antimicrobial surfaces and coatings in several industries. Antimicrobial coatings need to provide desirable attributes such as potent antibacterial efficacy, environmental safety, low toxicity, and ease of fabrication.

Antibacterial coatings may be of great interest to reduce or minimize biofouling on membrane surfaces used in water treatment applications. Typical adverse effects of membrane biofouling include (i) a reduction in membrane water flux, (ii) biodegradation and/or biodeterioration of the membrane surface (iii) development of human pathogens on membrane surfaces, (iv) increased energy requirements; this is due to the higher pressure requirements needed to overcome the biofilm resistance and the flux decline.<sup>98, 99</sup>

Effective prevention of microbial growth in a membrane system can be achieved by maintaining a sufficiently high concentration of chlorine. However, this may not be desirable based on environmental concerns and stricter legislative regulation corresponding to the discharge of chlorinated brines. Moreover, many materials are attacked by chlorine, so this treatment greatly limits the type of membranes that may be employed.

More effective and ecologically sound methods are needed to prevent or control the formation of biofilms on membrane surfaces. This need has led to the development of surface modification of membranes with polymers, <sup>101, 102</sup> and surface functionalization with silver, <sup>103-105</sup> quaternary ammonium groups, <sup>106, 107</sup> metals <sup>108, 109</sup> or chitosan <sup>110-112</sup>. In

P P

pr

de I :

sp<sub>e</sub>

The

this work, I exploit metal nanoparticle/polyelectrolyte films to create a new antifouling coating for membranes.

#### 1.5. Outline of the Thesis

Chapter 2 introduces a new approach for preparing catalytic metal nanoparticles encapsulated in PEMs. I examine the catalytic activity of Pd nanoparticles incorporated in poly(acrylic acid) (PAA)/polyethylenimine (PEI) films on alumina. In this case, alternating adsorption of PAA and a PEI-Pd(II) complex on alumina and subsequent reduction of Pd(II) by NaBH<sub>4</sub> yield catalytic Pd nanoparticles embedded in multilayer polyelectrolyte films. The chapter describes both the activity and remarkable selectivity of these Pd nanocatalysts during the hydrogenation of structurally similar unsaturated alcohols.

In Chapter 3, I first describe a modified LbL method for preparing immobilized Pd nanoparticles where catalytic Pd nanoparticles in multilayer polyelectrolyte films are prepared by alternating immersions of a substrate in PdCl<sub>4</sub><sup>2-</sup> and PEI solutions followed by chemical reduction of Pd(II) with NaBH<sub>4</sub>. Since only one polymer is used for the preparation of PEMs, the catalytic access to the Pd nanoparticles is high than in the films described in chapter 2. Since reduced PdCl<sub>4</sub><sup>2-</sup>/PEI system is not well-studied in literature, I first characterize these films using UV-visible spectroscopy, X-ray photoelectron spectroscopy, atomic absorption spectroscopy, and transmission electron microscopy, and compare the catalytic properties of these films with the system discussed in Chapter 2. The effect of the number of bilayers on the catalytic activity and selectivity is presented

to show the high accessibility of nanoparticle in reduced PdCl<sub>4</sub><sup>2</sup>/PEI films along with good catalytic selectivity.

Silver is known as one of the oldest antimicrobial agents. Silver ions are thought to inhibit bacterial enzymes and bind to DNA and have been used effectively against different bacteria, fungi and viruses. In Chapter 4, I discuss the application of silver nanoparticles incorporated in PEMs as antibacterial coating on polyether sulfone membranes. The mechanism of antibacterial action by the nanoparticles presumably involves slow release of Ag<sup>+</sup> ions, leading to sustained life of nanoparticle coatings compared to coatings containing Ag<sup>+</sup> ions. Leaching experiments with silver nanoparticles and ions indicate that the rate of leaching of silver nanoparticles is about an order of magnitude lower than that of silver ions.

In the last chapter of this thesis, I present the conclusions obtained from my research work and finally discuss some of the future prospects of my studies.

## 1.6 References

- 1. Rajan, M. Business Communications Company, Inc. 2001.
- 2. Valden, M.; Lai, X.; Goodman, D. W. Science 1998, 281, (5383), 1647-1650.
- 3. Decher, G. Science 1997, 277, (5330), 1232-1237.
- 4. Decher, G.; Eckle, M.; Schmitt, J.; Struth, B. Current Opinion in Colloid & Interface Science 1998, 3, (1), 32-39.
- 5. Decher, G.; Hong, J. D. Berichte der Bunsen-Gesellschaft 1991, 95, (11), 1430-4.
- 6. Hammond, P. T. Current Opinion in Colloid & Interface Science 2000, 4, (6), 430-442.
- 7. Nolte, M.; Doench, I.; Fery, A. ChemPhysChem **2006**, 7, (9), 1985-1989.
- 8. Zhang, S.; Yang, W.; Niu, Y.; Li, Y.; Zhang, M.; Sun, C. Analytical and Bioanalytical Chemistry 2006, 384, (3), 736-741.
- 9. Yang, X.; Johnson, S.; Shi, J.; Holesinger, T.; Swanson, B. Sensors and Actuators, B: Chemical 1997, B45, (2), 87-92.
- 10. Kerdjoudj, H.; Boura, C.; Marchal, L.; Dumas, D.; Schaff, P.; Voegel, J. C.; Stoltz, J. F.; Menu, P. *Bio-Medical Materials and Engineering* **2006**, 16, (Suppl. 4), S123-S129.
- 11. Zhu, H.; Ji, J.; Shen, J. Biomacromolecules **2004**, 5, (5), 1933-1939.
- 12. Liang, Z.; Wang, C.; Tong, Z.; Ye, W.; Ye, S. Reactive & Functional Polymers **2005**, 63, (1), 85-94.
- 13. Caruso, F.; Moehwald, H. Journal of the American Chemical Society 1999, 121, (25), 6039-6046.

- 14. Kujawa, P.; Sanchez, J.; Badia, A.; Winnik, F. M. Journal of Nanoscience and Nanotechnology **2006**, 6, (6), 1565-1574.
- 15. Choi, J.; Rubner, M. F. *Macromolecules* **2005**, 38, (1), 116-124.
- 16. Burke, S. E.; Barrett, C. J. *Macromolecules* **2004**, 37, (14), 5375-5384.
- 17. Kim, B. Y.; Bruening, M. L. *Langmuir* **2003**, 19, (1), 94-99.
- 18. Schneider, A.; Picart, C.; Senger, B.; Schaaf, P.; Voegel, J.-C.; Frisch, B. *Langmuir* **2007**, 23, (5), 2655-2662.
- 19. Blomberg, E.; Poptoshev, E.; Caruso, F. Langmuir 2006, 22, (9), 4153-4157.
- 20. Jomaa, H. W.; Schlenoff, J. B. *Macromolecules* **2005**, 38, (20), 8473-8480.
- 21. Tjipto, E.; Quinn, J. F.; Caruso, F. *Langmuir* **2005**, 21, (19), 8785-8792.
- 22. Tan, H. L.; McMurdo, M. J.; Pan, G.; Van Patten, P. G. Langmuir 2003, 19, (22), 9311-9314.
- 23. Steitz, R.; Leiner, V.; Tauer, K.; Khrenov, V.; Klitzing, R. V. Applied Physics A: Materials Science & Processing 2002, 74, (Suppl., Pt. 1), S519-S521.
- 24. Miller, M. D.; Bruening, M. L. Chemistry of Materials 2005, 17, (21), 5375-5381.
- 25. Dong, W.-F.; Liu, S.; Wan, L.; Mao, G.; Kurth, D. G.; Moehwald, H. Chemistry of Materials 2005, 17, (20), 4992-4999.
- 26. Bucur, C. B.; Sui, Z.; Schlenoff, J. B. *Journal of the American Chemical Society* **2006**, 128, (42), 13690-13691.
- 27. Keller, S. W.; Johnson, S. A.; Yonemoto, E. H.; Brigham, E. S.; Saupe, G. B.; Mallouk, T. E. *Advances in Chemistry Series* **1998**, 254, (Photochemistry and Radiation Chemistry), 359-379.

- 28. Laurent, D.; Schlenoff, J. B. Langmuir 1997, 13, (6), 1552-1557.
- 29. Komarala, V. K.; Rakovich, Y. P.; Bradley, A. L.; Byrne, S. J.; Corr, S. A.; Gun'ko, Y. K. *Nanotechnology* **2006**, 17, (16), 4117-4122.
- 30. Lowman, G. M.; Nelson, S. L.; Graves, S. M.; Strouse, G. F.; Buratto, S. K. Langmuir **2004**, 20, (6), 2057-2059.
- 31. Wang, D.; Rogach, A. L.; Caruso, F. Nano Letters 2002, 2, (8), 857-861.
- 32. Fredin, N. J.; Zhang, J.; Lynn, D. M. *Langmuir* **2007**, 23, (5), 2273-2276.
- 33. Jewell, C. M.; Zhang, J.; Fredin, N. J.; Wolff, M. R.; Hacker, T. A.; Lynn, D. M. *Biomacromolecules* **2006**, 7, (9), 2483-2491.
- 34. Ren, K.; Ji, J.; Shen, J. *Biomaterials* **2006**, 27, (7), 1152-1159.
- 35. Yoo, P. J.; Nam, K. T.; Qi, J.; Lee, S.-K.; Park, J.; Belcher, A. M.; Hammond, P. T. *Nature Materials* **2006**, 5, (3), 234-240.
- 36. Fischlechner, M.; Toellner, L.; Messner, P.; Grabherr, R.; Donath, E. Angewandte Chemie, International Edition 2006, 45, (5), 784-789.
- 37. Feldheim, D. L.; Grabar, K. C.; Natan, M. J.; Mallouk, T. E. *Journal of the American Chemical Society* **1996**, 118, (32), 7640-7641.
- 38. Keller, S. W.; Johnson, S. A.; Brigham, E. S.; Yonemoto, E. H.; Mallouk, T. E. Journal of the American Chemical Society 1995, 117, (51), 12879-80.
- 39. Leguen, E.; Chassepot, A.; Decher, G.; Schaaf, P.; Voegel, J.-C.; Jessel, N. Biomolecular Engineering 2007, 24, (1), 33-41.
- 40. Haynie, D. T.; Zhang, L.; Zhao, W.; Rudra, J. S. *Nanomedicine* **2006**, 2, (3), 150-157.
- 41. Kovacevic, D.; Glavanovic, S.; Peran, N. Colloids and Surfaces, A: Physicochemical and Engineering Aspects 2006, 277, (1-3), 177-182.

- 42. Salloum, D. S.; Schlenoff, J. B. *Biomacromolecules* **2004**, **5**, (3), 1089-1096.
- 43. Zhang, X.; Sun, Y.; Shen, J. *Protein Architecture* **2000**, 229-249.
- 44. Hamlin, R. E.; Dayton, T. L.; Johnson, L. E.; Johal, M. S. *Langmuir* **2007**, 23, (8), 4432-4437.
- 45. Shi, L.; Sun, J.; Liu, J.; Shen, J.; Gao, M. Chemistry Letters 2002, (12), 1168-1169.
- 46. Lvov, Y.; Caruso, F. Analytical Chemistry **2001**, 73, (17), 4212-4217.
- 47. Caruso, F.; Schuler, C. *Langmuir* **2000**, 16, (24), 9595-9603.
- 48. Recksiedler, C. L.; Deore, B. A.; Freund, M. S. *Langmuir* **2006**, 22, (6), 2811-2815.
- 49. Etienne, O.; Gasnier, C.; Taddei, C.; Voegel, J.-C.; Aunis, D.; Schaaf, P.; Metz-Boutigue, M.-H.; Bolcato-Bellemin, A.-L.; Egles, C. *Biomaterials* **2005**, 26, (33), 6704-6712.
- 50. Boulmedais, F.; Frisch, B.; Etienne, O.; Lavalle, P.; Picart, C.; Ogier, J.; Voegel, J. C.; Schaaf, P.; Egles, C. *Biomaterials* **2004**, 25, (11), 2003-2011.
- 51. Iler, R. K. Journal of Colloid and Interface Science 1966, 21, (6), 569-94.
- 52. Lee, L. L.; Chan, C. K.; Ngiam, M.; Ramakrishna, S. Nano 2006, 1, (2), 101-113.
- 53. Quinn, B. M.; Liljeroth, P.; Ruiz, V.; Laaksonen, T.; Kontturi, K. *Journal of the American Chemical Society* **2003**, 125, (22), 6644-6645.
- 54. Suzdalev, I. P.; Suzdalev, P. I. Russian Chemical Reviews **2001**, 70, (3), 177-210.
- 55. Chen, S.; Ingrma, R. S.; Hostetler, M. J.; Pietron, J. J.; Murray, R. W.; Schaaff, T. G.; Khoury, J. T.; Alvarez, M. M.; Whetten, R. L. Science 1998, 280, (5372), 2098-2101.

- 56. Alvarez, M. M.; Khoury, J. T.; Schaaff, T. G.; Shafigullin, M. N.; Vezmar, I.; Whetten, R. L. *Journal of Physical Chemistry B* **1997**, 101, (19), 3706-3712.
- 57. Li, Y.; Boone, E.; El-Sayed, M. A. Langmuir 2002, 18, (12), 4921-4925.
- 58. Schmid, G. Nanoscale Materials in Chemistry 2001, 15-59.
- 59. Rao, C. N. R.; Kulkarni, G. U.; Thomas, P. J.; Edwards Peter, P. Chemistry 2002, 8, (1), 28-35.
- 60. Li, Y.; El-Sayed, M. A. Journal of Physical Chemistry B 2001, 105, (37), 8938-8943.
- 61. Niu, Y.; Yeung, L. K.; Crooks, R. M. *Journal of the American Chemical Society* **2001**, 123, (28), 6840-6846.
- 62. Park, J. H.; Lim, Y. T.; Park, O. O.; Kim, J. K.; Yu, J.-W.; Kim, Y. C. Chemistry of Materials 2004, 16, (4), 688-692.
- 63. Lee, J.-E.; Kim, J.-W.; Jun, J.-B.; Ryu, J.-H.; Kang, H.-H.; Oh, S.-G.; Suh, K.-D. Colloid and Polymer Science **2004**, 282, (3), 295-299.
- 64. Ye, J.-S.; Ottova, A.; Tien, H. T.; Sheu, F.-S. *Bioelectrochemistry* **2003**, 59, (1-2), 65-72.
- 65. Liu, Z.; Ling, X. Y.; Su, X.; Lee, J. Y. Journal of Physical Chemistry B 2004, 108, (24), 8234-8240.
- 66. Mallick, K.; Scurrell, M. S. Applied Catalysis, A: General 2003, 253, (2), 527-536.
- 67. Barea, E.; Batlle, X.; Bourges, P.; Corma, A.; Fornes, V.; Labarta, A.; Puntes, V. F. *Journal of the American Chemical Society* **2005**, 127, (51), 18026-18030.
- 68. Riahi, G.; Guillemot, D.; Polisset-Thfoin, M.; Khodadadi, A. A.; Fraissard, J. Catalysis Today 2002, 72, (1-2), 115-121.

- 69. Bonder, M. J.; Zhang, Y.; Kiick, K. L.; Papaefthymiou, V.; Hadjipanayis, G. C. Journal of Magnetism and Magnetic Materials 2007, 311, (2), 658-664.
- 70. Mei, Y.; Lu, Y.; Polzer, F.; Ballauff, M.; Drechsler, M. Chemistry of Materials **2007**, 19, (5), 1062-1069.
- 71. Hsieh, S.-N.; Wen, T.-C.; Guo, T.-F. *Materials Chemistry and Physics* **2007**, 101, (2-3), 383-386.
- 72. Park, M. J.; Park, J.; Hyeon, T.; Char, K. Journal of Polymer Science, Part B: Polymer Physics 2006, 44, (24), 3571-3579.
- 73. Kraemer, M.; Perignon, N.; Haag, R.; Marty, J.-D.; Thomann, R.; Lauth-de Viguerie, N.; Mingotaud, C. *Macromolecules* **2005**, 38, (20), 8308-8315.
- 74. Panziera, N.; Pertici, P.; Barazzone, L.; Caporusso, A. M.; Vitulli, G.; Salvadori, P.; Borsacchi, S.; Geppi, M.; Veracini, C. A.; Martra, G.; Bertinetti, L. *Journal of Catalysis* **2007**, 246, (2), 351-361.
- 75. Song, R. G.; Yamaguchi, M.; Nishimura, O.; Suzuki, M. *Applied Surface Science* **2007**, 253, (6), 3093-3097.
- 76. Astruc, D.; Lu, F.; Aranzaes, J. R. Angewandte Chemie, International Edition **2005**, 44, (48), 7852-7872.
- 77. Lu, F.; Ruiz, J.; Astruc, D. Tetrahedron Letters 2004, 45, (51), 9443-9445.
- 78. Nasar, K.; Fache, F.; Lemaire, M.; Beziat, J. C.; Besson, M.; Gallezot, P. Journal of Molecular Catalysis 1994, 87, (1), 107-15.
- 79. Bonnemann, H.; Braun, G. A. Chemistry--A European Journal 1997, 3, (8), 1200-1202.
- 80. Tamura, M.; Fujihara, H. *Journal of the American Chemical Society* **2003**, 125, (51), 15742-15743.
- 81. Jansat, S.; Gomez, M.; Philippot, K.; Muller, G.; Guiu, E.; Claver, C.; Castillon, S.; Chaudret, B. *Journal of the American Chemical Society* **2004**, 126, (6), 1592-1593.

- 82. Leger, B.; Nowicki, A.; Roucoux, A.; Rolland, J.-P. *Journal of Molecular Catalysis A: Chemical* **2007**, 266, (1-2), 221-225.
- 83. Tada, M.; Bal, R.; Namba, S.; Iwasawa, Y. Applied Catalysis, A: General 2006, 307, (1), 78-84.
- 84. Mu, X.-d.; Evans, D. G.; Kou, Y. Catalysis Letters 2004, 97, (3-4), 151-154.
- 85. Sulman, E.; Bronstein, L.; Matveeva, V.; Sulman, M.; Lakina, N.; Doluda, V.; Valetsky, P. *Nanocatalysis* **2006**, 51-98.
- 86. Zhao, M.; Crooks, R. M. Advanced Materials 1999, 11, (3), 217-220.
- 87. Kramer, A.; Kremer, J.; Assadian, O.; Schneider, I.; Daehne, H.; Schwemmer, J.; Mueller, G.; Siegmund, W.; Jaekel, C. *International Journal of Clinical Pharmacology and Therapeutics* **2006**, 44, (12), 677-692.
- 88. Ohkawa, H.; Tsuji, M.; Ohtsuki, K.; Ohnishi, M.; Akitsu, T. Plasma Processes and Polymers 2005, 2, (2), 112-119.
- 89. Tsou, T.-L.; Tang, S.-T.; Huang, Y.-C.; Wu, J.-R.; Young, J.-J.; Wang, H.-J. Journal of Materials Science: Materials in Medicine 2005, 16, (2), 95-100.
- 90. Shekhar, N.; Bhattacharya, D.; Kumar, D.; Gupta, R. K. Canadian Journal of Microbiology 2006, 52, (9), 805-808.
- 91. Kim, S.; Kim, H.-J. International Biodeterioration & Biodegradation **2006**, 57, (3), 155-162.
- 92. Fijan, S.; Koren, S.; Cencic, A.; Sostar-Turk, S. Diagnostic Microbiology and Infectious Disease 2007, 57, (3), 251-257.
- 93. Vaelimaa, A.-L.; Honkalampi-Haemaelaeinen, U.; Pietarinen, S.; Willfoer, S.; Holmbom, B.; von Wright, A. *International Journal of Food Microbiology* **2007**, 115, (2), 235-243.
- 94. Gaikowski Mark, P.; Wolf Jeffrey, C.; Endris Richard, G.; Gingerich William, H. *Toxicologic pathology* **2003**, 31, (6), 689-97.

- 95. O'Toole, G. A.; Stewart, P. S. Nature Biotechnology 2005, 23, (11), 1378-1379.
- 96. Hoffman, L. R.; D'Argenio, D. A.; MacCoss, M. J.; Zhang, Z.; Jones, R. A.; Miller, S. I. *Nature* **2005**, 436, (7054), 1171-1175.
- 97. Khardori, N.; Yassien, M. Journal of Industrial Microbiology 1995, 15, (3), 141-7.
- 98. Al-Ahmad, M.; Aleem, F. A. A.; Mutiri, A.; Ubaisy, A. *Desalination* **2000**, 132, (1-3), 173-179.
- 99. Ridgway, H.; Ishida, K.; Rodriguez, G.; Safarik, J.; Knoell, T.; Bold, R. Methods in Enzymology 1999, 310, (Biofilms), 463-494.
- 100. Flemming, H.-C. Experimental Thermal and Fluid Science 1997, 14, (4), 382-391.
- 101. Cheng, Z.; Zhu, X.; Shi, Z. L.; Neoh, K. G.; Kang, E. T. Surface Review and Letters **2006**, 13, (2&3), 313-318.
- 102. Kochkodan, V. M.; Hilal, N.; Goncharuk, V. V.; Al-Khatib, L.; Levadna, T. I. *Colloid Journal* **2006**, 68, (3), 267-273.
- 103. Dai, J.; Bruening, M. L. Nano Letters **2002**, 2, (5), 497-501.
- 104. Gray, J. E.; Norton, P. R.; Alnouno, R.; Marolda, C. L.; Valvano, M. A.; Griffiths, K. *Biomaterials* **2003**, 24, (16), 2759-2765.
- 105. Grunlan, J. C.; Choi, J. K.; Lin, A. Biomacromolecules 2005, 6, (2), 1149-1153.
- 106. Cen, L.; Neoh, K. G.; Kang, E. T. *Langmuir* **2003**, 19, (24), 10295-10303.
- 107. Nakagawa, Y.; Hayashi, H.; Tawaratani, T.; Kourai, H.; Horie, T.; Shibasaki, I. Applied and Environmental Microbiology 1984, 47, (3), 513-18.
- 108. Fu, G.; Vary, P. S.; Lin, C.-T. Journal of Physical Chemistry B 2005, 109, (18), 8889-8898.

- 109. Stoimenov, P. K.; Klinger, R. L.; Marchin, G. L.; Klabunde, K. J. *Langmuir* **2002**, 18, (17), 6679-6686.
- 110. Fu, J.; Ji, J.; Yuan, W.; Shen, J. Biomaterials 2005, 26, (33), 6684-6692.
- 111. Huh, M. W.; Kang, I.-K.; Lee, D. H.; Kim, W. S.; Lee, D. H.; Park, L. S.; Min, K. E.; Seo, K. H. *Journal of Applied Polymer Science* **2001**, 81, (11), 2769-2778.
- 112. Lim, S.-H.; Hudson, S. M. *Journal of Macromolecular Science, Polymer Reviews* **2003**, C43, (2), 223-269.

# Chapter 2: Selective Hydrogenation By Pd Nanoparticles Embedded In Poly(Acrylic Acid)/Polyethyleneimine Multilayers

# 2.1. Introduction

Metal nanoparticles are an interesting class of materials because they often exhibit different properties than the corresponding bulk metals.<sup>1-5</sup> For example, bulk Au is not catalytically active, but recent studies have shown that Au nanoparticles can serve as catalysts for oxidation and hydrogenation reactions.<sup>6-9</sup> Additionally, nanoparticle properties can be tuned by varying their sizes<sup>8, 10, 11</sup> and environments.<sup>12</sup> Because of these unique characteristics, metal nanoparticles are being intensively studied for applications in catalysis, <sup>10, 13</sup> optoelectronics, <sup>14</sup> preservatives, <sup>15</sup> and biosensing <sup>16</sup>.

Metal nanoparticles are particularly attractive for catalysis because their large surface area-to-volume ratio allows effective utilization of expensive metals.<sup>4, 17</sup> Moreover, variation of nanoparticle size sometimes allows control over catalytic activity.<sup>10</sup> Unfortunately, however, aggregation of naked nanoparticles often prohibits tailoring of particle size.<sup>18</sup> To overcome this problem, catalytic nanoparticles have been immobilized on solid supports (e.g., carbon, metal oxides, and zeolites) or stabilized by capping with ligands ranging from small organic molecules to large polymers.<sup>5-7</sup> Recently, novel systems such as dendrimers,<sup>19</sup> block copolymer nanospheres,<sup>20</sup> and crosslinked lyotropic liquid crystals<sup>10</sup> were employed to encapsulate metal nanoparticles.

Multilayer polyelectrolyte films (MPFs) are especially attractive for encapsulating metal nanoparticles because their layer-by-layer deposition is both convenient and versatile. We are developing catalytic nanoparticles embedded in multilayered polyelectrolyte films because the layer-by-layer deposition of these coatings, which

simply involves alternating adsorption of polycations and polyanions, offers a versatile platform for potentially controlling catalyst properties. <sup>21-23</sup> There are two main strategies for preparing nanoparticle-containing polyelectrolyte films. In the first, the nanoparticles serve as the polycation or polyanion during film deposition, <sup>24, 25</sup> while in the second, metal ions are incorporated into polyelectrolyte films and subsequently reduced to form nanoparticles (Scheme 2.1). <sup>26, 27</sup> Either way, the simple layer-by-layer procedure permits deposition of films on nearly any surface, thus allowing the formation of catalytic systems on recoverable, high-surface-area substrates such as alumina. Moreover, because nearly any highly charged material can be used in alternating polyelectrolyte deposition, variation of constituent polyelectrolytes should allow tailoring of the nanoparticle environment as well as control over access to catalytic particles.

This chapter will discuss the use of Pd nanoparticles embedded in polyelectrolyte multilayer films, [poly(acrylic acid) (PAA)/polyethyleneimine (PEI)]<sub>n</sub> films in particular, as selective catalysts during hydrogenation of structurally similar alcohols. Pd nanoparticles encapsulated in polymer films are not only active, but also selective during hydrogenation reactions. Nanoparticles in [PAA/PEI-Pd(0)]<sub>3.5</sub>PAA films can catalyze hydrogenation of allyl alcohol at a rate that is an order of magnitude faster than hydrogenation of 3-methyl-1-penten-3-ol. Studies of transport in diffusion dialysis experiments suggest that differential rates of transport to the Pd nanoparticles may account for the selectivities. First-order reaction rates are also consistent with diffusion-limited kinetics.

# 2.2. Experimental Section

#### 2.2.1. Materials

Polyethyleneimine (PEI) ( $M_w = 25~000~\text{Da}$ ), poly(acrylic acid) (PAA) (25 wt % in water,  $M_w = 90~000~\text{Da}$ ), poly(styrene sulfonate) (PSS) (sodium salt,  $M_w = 125~000~\text{Da}$ ), palladium (5 wt % on alumina powder),  $\alpha$ -alumina (100 mesh, typical particle size 75-100  $\mu$ m), allyl alcohol (99%), 1-penten-3-ol (99%), and 3-methyl-1-penten-3-ol (99%) were purchased from Aldrich. Potassium tetrachloropalladate(II) (99.99%) was obtained from Alfa Aesar, and sodium borohydride was acquired from Spectrum. All reagents were used as received, and solutions were prepared with deionized water (Milli-Q, 18.2 M $\Omega$  cm).

# 2.2.2. Preparation of Pd Nanoparticles Encapsulated in PAA/PEI multilayer films

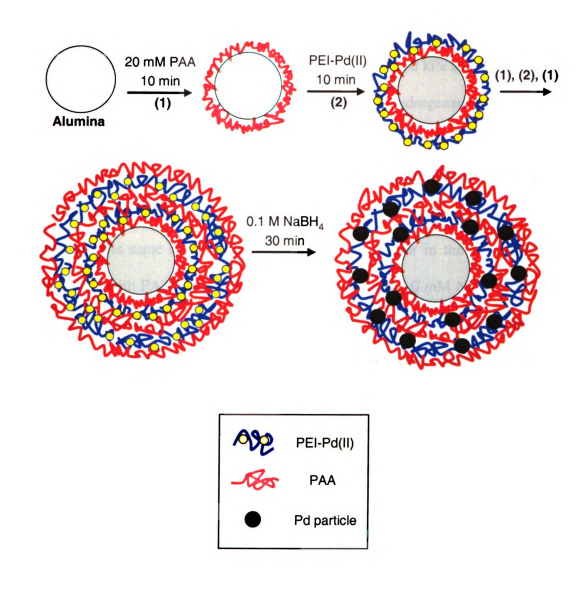
Synthesis of [PAA/PEI-Pd(0)]<sub>n</sub>PAA films occurs through alternating immersions of alumina particles in solutions of PAA and a PEI-Pd(II) complex, followed by reduction of Pd(II) by NaBH<sub>4</sub> to give catalytic Pd nanoparticles in a PAA/PEI film (Scheme 2.1). Specifically, 15 g of α-alumina was mixed with 100 mL of a solution containing 20 mM PAA (pH adjusted to 4.0), and the suspension was stirred vigorously for 10 min. Subsequently, the alumina was allowed to settle, and the supernatant was decanted. The alumina particles were then washed with three 100-mL aliquots of deionized water to remove any excess PAA. To deposit a PEI-Pd(II) layer, 100 mL of a PEI-Pd(II) complex (1 mg/mL PEI, 2 mM K<sub>2</sub>PdCl<sub>4</sub>, pH adjusted to 9.0) was added to the PAA-coated alumina, and the particles were stirred for 10 min and washed as described above. Subsequent bilayers were deposited similarly Reduction of Pd(II) in these films was effected by exposure of the coated alumina to 100 mL of fresh 1 mM NaBH4 for 30

min (with stirring). The reduced films were washed three times with water after exposure to NaBH<sub>4</sub>. Films were always capped with PAA and rinsed between the depositions of each polyelectrolyte. All the catalysts were vacuum-dried after NaBH<sub>4</sub> reduction, and no flocculation of the alumina was observed during deposition and rinsing. The coated alumina easily dispersed upon exposure to hydrogenation solutions.

# 2.2.3. Characterization of Pd Nanoparticles

Reduced [PAA/PEI-Pd(II)]<sub>3</sub>PAA films were also deposited on carbon-coated copper grids for transmission electron microscopy (TEM). Prior to film deposition, the grids were cleaned in a UV/ozone cleaner for 1 min, and TEM was performed on a JEOL 100CX microscope using an accelerating voltage of 100 kV. The digital images were taken with a Mega View III Soft Imaging System. Films were prepared using alternating 5-min immersions in PAA and PEI-Pd(II) solutions with 1-min water rinses between polycation and polyanion depositions. Nanoparticles formed upon reduction with 0.1 M NaBH<sub>4</sub> for 15 min. We used somewhat shorter deposition times than those employed for the catalyst synthesis because of the small surface area of the TEM grid.

UV-Visible absorption spectra of [PEI-Pd(II)/PAA]<sub>n</sub> films on quartz slides were obtained using a Perkin-Elmer UV/Vis (model Lambda 40) spectrophotometer. To form films on quartz, slides were alternatively immersed into PEI-Pd(II)-complex and PAA solutions for 10 min each, with a 1-min water rinse after each deposition. These depositions began with PEI-Pd(II) rather than PAA because quartz is negatively charged at the pH values used in deposition.



Scheme 2.1. Formation of Nanoparticles in PEMs

# 2.2.4. Hydrogenation Reactions

Catalytic hydrogenations were run in a 200-mL, 3-neck, round-bottomed flask. H<sub>2</sub> was bubbled through a frit at the bottom of the solution at 50 kPa and the solution was vigorously stirred throughout the reaction. The aqueous hydrogenation solutions (200 mL) initially contained 2.0 mmol of substrate and either 10 mg of commercial palladium catalyst (5 wt% Pd on alumina powder, Aldrich) or 250 mg of alumina coated with 3.5 bilayers of PAA/PEI-Pd(0). (The amounts of catalyst were chosen to achieve approximately the same quantity of Pd loading in the reactor in the two cases.) The alumina coated with PAA/PEI-Pd(II) was treated with fresh 1.0 mM NaBH4 and washed 3 times with water before the hydrogenation reaction to ensure that all of the Pd was reduced. (Nanoparticles may oxidize over time, and this second reduction step seemed necessary to maintain catalyst activity.) Suspensions of catalyst in H<sub>2</sub>O were bubbled with  $H_2$  for 30 min before adding the substrates, all of which were liquids. Gas chromatography (Shimadzu GC-17A equipped with an RTx-BAC1 column) was used to monitor the reactions. The sensitivity of the flame-ionization detector was assumed to be the same for products and reactants because they contain the same number of carbon atoms. This has been verified in several cases. For reactions with more than one product, GC-MS and <sup>1</sup>H NMR were used to identify the products. Turnover frequencies were calculated from the slopes of the linear portions of plots of percent hydrogenation versus time. Slopes were determined by forcing the intercept to be zero except in the case of commercial catalyst coated with 3.5 PAA/PEI bilayers. In that case, the intercept was not forced to be zero because of a small offset that occurred primarily with allyl alcohol. Fitting the intercept rather than forcing the fit through zero resulted in only

small (<25%) changes in selectivity and a 35% decrease in the turnover frequency for allyl alcohol.

### 2.2.5. Determination of the Amount of Pd in Catalysts

To calculate turnover frequencies, the amount of Pd in the catalyst must be known. For both the commercial and synthesized catalysts, the percentage of palladium in the material was determined by atomic emission spectroscopy. Standard solutions (0.1 to 0.5 mM) were prepared by dissolving K<sub>2</sub>PdCl<sub>4</sub> in 0.1 M HNO<sub>3</sub>, and sample solutions were prepared by stirring 250 mg of synthesized catalyst or 10 mg of commercial catalyst in 2 mL of *aqua regia* for 15 min. The solutions were diluted to 12 mL and centrifuged (the α-alumina support does not dissolve in *aqua regia*), and the supernatant was analyzed using its emission at 633 nm. The amounts of Pd in 250 mg of 3.5-bilayer PAA/PEI-Pd(0) on alumina and 10 mg of 5% Pd-on-alumina were 3.3x10<sup>-6</sup> and 5.3x10<sup>-6</sup> moles, respectively. The amount in the commercial catalyst corresponds to 5.6 wt%, and the manufacturer reported 5 wt%.

# 2.2.6. Determination of Transport Rates by Diffusion Dialysis

A home-built diffusion dialysis set-up was used to study the transport of unsaturated alcohols through polyelectrolyte multilayer films. The apparatus consists of two glass cells (100 mL) between which a 0.02 µm alumina membrane (Anodisc<sup>™</sup>) coated with (PAA/PEI)<sub>7</sub> film, was sandwiched as shown in Figure 2.1.<sup>28-30</sup> The feed side of the glass cell initially contained 20 mM of the unsaturated alcohol (allyl alcohol, penten-1-ol or 3-methyl penten-1-ol), while the permeate side contained pure water. The

feed and permeate sides were both stirred continuously to minimize concentration polarization at the membrane interface. Aliquots of samples were taken from the permeate side at regular intervals of time, and were then analyzed by GC to determine the rate of transport through the coated membrane.

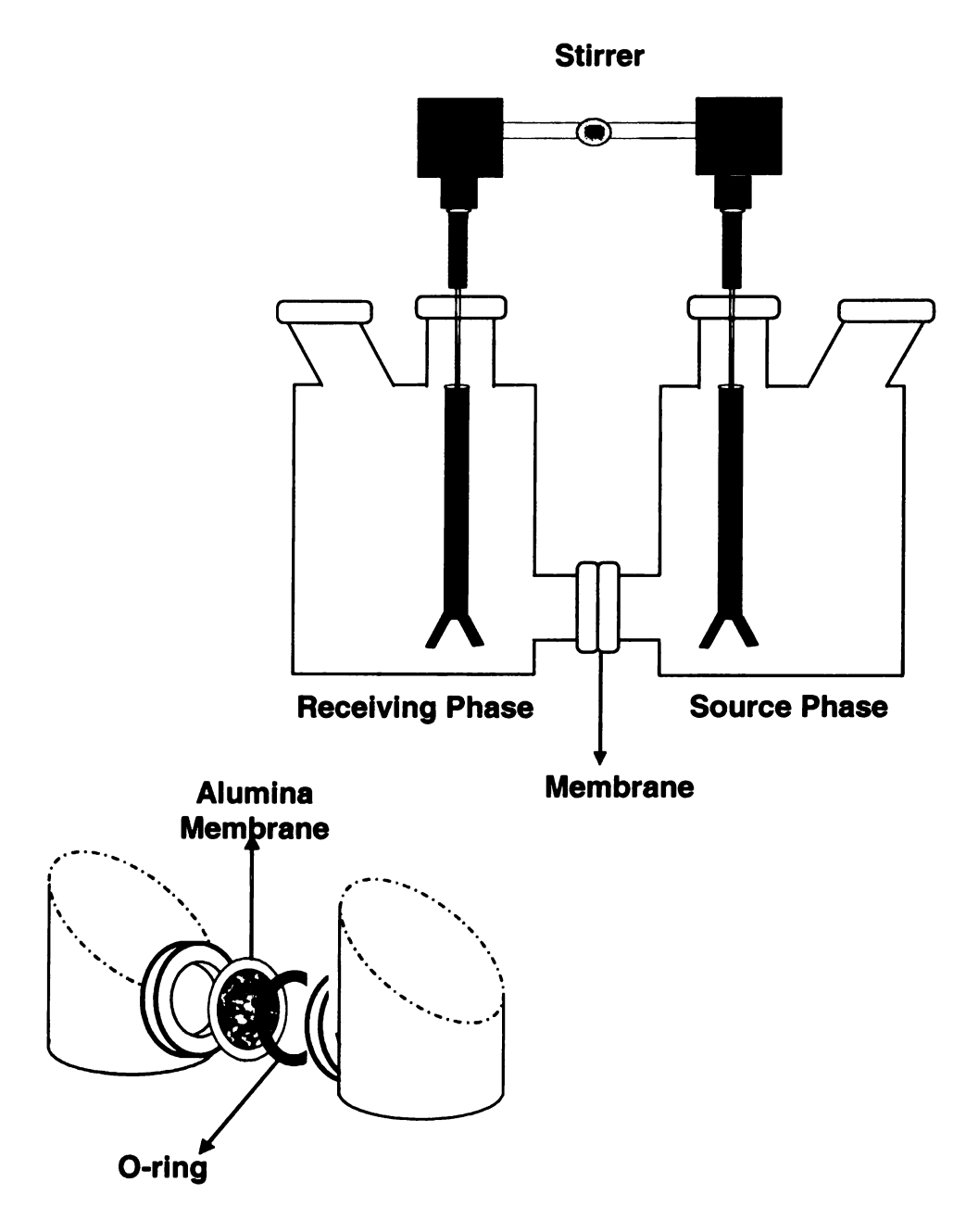


Figure 2.1. Home-built diffusion dialysis set-up for transport experiments (Figure courtesy of Dr. Jinhua Dai)

#### 2.3. Results and Discussion

#### 2.3.1. Film Deposition

In investigation of catalysis by nanoparticle-containing films, it is important to first understand film growth and composition. We performed UV/Vis spectroscopy of [PEI-Pd(II)/PAA]<sub>n</sub> films on quartz to demonstrate that layer-by-layer deposition occurs. As shown in Figure 2.2, the absorbance of PEI-Pd(II)/PAA films at 222 nm, which is likely due to a Pd(II)-amine charge transfer band, <sup>13, 31</sup> increases linearly with the number of bilayers.

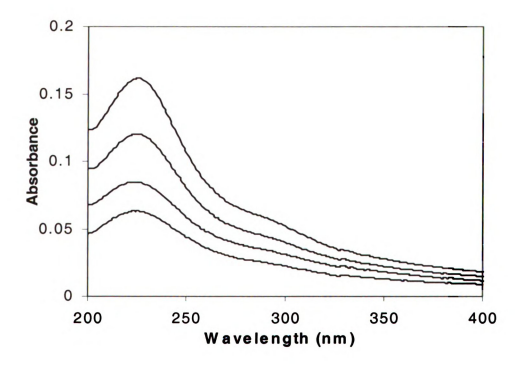


Figure 2.2. UV-Vis absorption spectra of [PEI-Pd(II)/PAA]<sub>n</sub>PEI-Pd(II) films on quartz substrates with n = 0, 1, 2, and 3 (from lower to upper curves).

#### 2.3.2. Film Characterization

To investigate the reduction of Pd(II) to form nanoparticles, we performed TEM of films deposited on the Cu-coated TEM grid. The TEM image in Figure 2.3 confirms the formation of Pd nanoparticles during exposure of [PAA/PEI-Pd(II)]<sub>3</sub>PAA films to NaBH<sub>4</sub>. The particles have diameters of 1-3 nm and are distributed throughout the film. (We note that there may be particles with diameters <1 nm, but these would be difficult to see and likely unstable.)

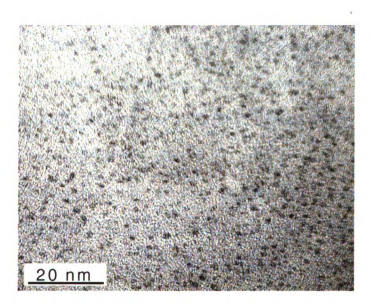


Figure 2.3. TEM image of [PAA/PEI-Pd(0)]PAA on a carbon-coated copper grid.

#### 2.3.3. Selective Catalysis of Hydrogenation

To show that encapsulation of Pd nanoparticles in polyelectrolyte films can result in selective catalysis, we hydrogenated a series of unsaturated alcohols using PAA/PEI-Pd(0) films on alumina particles as well as a commercial Pd-on-alumina catalyst. Table 2.1 summarizes the turnover frequencies (TOFs) for aqueous hydrogenation of allyl

alcohol (1), 1-penten-3-ol (2), and 3-methyl-1-penten-3-ol (3), which differ only in the substituents at the  $\alpha$ -carbon of the double bond.

On "naked" 5% Pd-on-alumina catalyst (Table 2.1, column 2), the reaction rates for 1, 2, and 3 are very close ( $1/2 \approx 1/3 \approx 0.87$ ), showing that the presence of additional alkyl groups at the  $\alpha$ -carbon does not have a significant effect on reactivity. However, for alumina coated with [PAA/PEI-Pd(0)]<sub>3</sub>PAA (3.5 bilayers of film, Table 2.1, column 3), the initial rate for hydrogenation of 1 is 3- and 12-fold faster than that for 2 and 3, respectively. Figure 2.4 indicates the amount of substrate hydrogenated as a function of reaction time for 1, 2, and 3 using [PAA/PEI-Pd(0)]<sub>3</sub>PAA-coated alumina as a catalyst.

To further improve selectivity, we capped two bilayers of PAA/PEI-Pd(0) with five bilayers of PAA/PEI (without any Pd). With the capping layers, selectivity for 1 over 3 increases to 24 (Table 2.1, column 5). The presence of the capping layers decreases the hydrogenation rate for all of the alcohols, but hydrogenation of 3 is most attenuated. This likely results from very slow diffusion of 3 through the film (see below). We also carried out the hydrogenation in a 4:1 methanol-water mixture because hydrogen and the unsaturated alcohols (particularly 2 and 3) are more soluble in organic solvents than in water. The rate of hydrogenation of 1 is 40% lower in 80% methanol than in pure water, but selectivities are 60-80% higher (Table 2.1, column 4). The increased selectivity and decreased rate probably result from less swelling of the film in the methanol-water mixture. These selectivities are, in general, about 2-3-fold higher than those reported for dendrimer-encapsulated Pd nanoparticles, suggesting that the polyelectrolyte films provide highly restricted access to catalytic sites of nanoparticles.<sup>21</sup>

**Table 2.1**. Turnover Frequencies (TOFs) for hydrogenation of structurally related unsaturated alcohols by several Pd catalysts.

	TOF (moles hydrogenated per mol Pd per h)				
Substrate	5% Pd on alumina	3.5-bilayer PAA/PEI- Pd(0) <sup>a</sup>	3.5-bilayer PAA/PEI- Pd(0) <sup>b</sup>	7 bilayers <sup>c</sup>	Coated 5% Pd on alumina <sup>d</sup>
1OH	1300±150	727±128	435±64	141±20	33±5
2/\OH	1500±120	278±23	94±7	65±8	15±3
3 OH	1500±100	60±15	23±4	6±1	7±1

<sup>&</sup>lt;sup>a</sup> Hydrogenation carried out in deionized water.

<sup>&</sup>lt;sup>b</sup> Hydrogenation carried out in methanol-water (4:1 v:v).

<sup>&</sup>lt;sup>c</sup> 2 bilayers of PAA/PEI-Pd(0) capped with 5 bilayers of PAA/PEI.

<sup>&</sup>lt;sup>d</sup> 3.5 bilayers of PAA/PEI deposited on 5% Pd on alumina

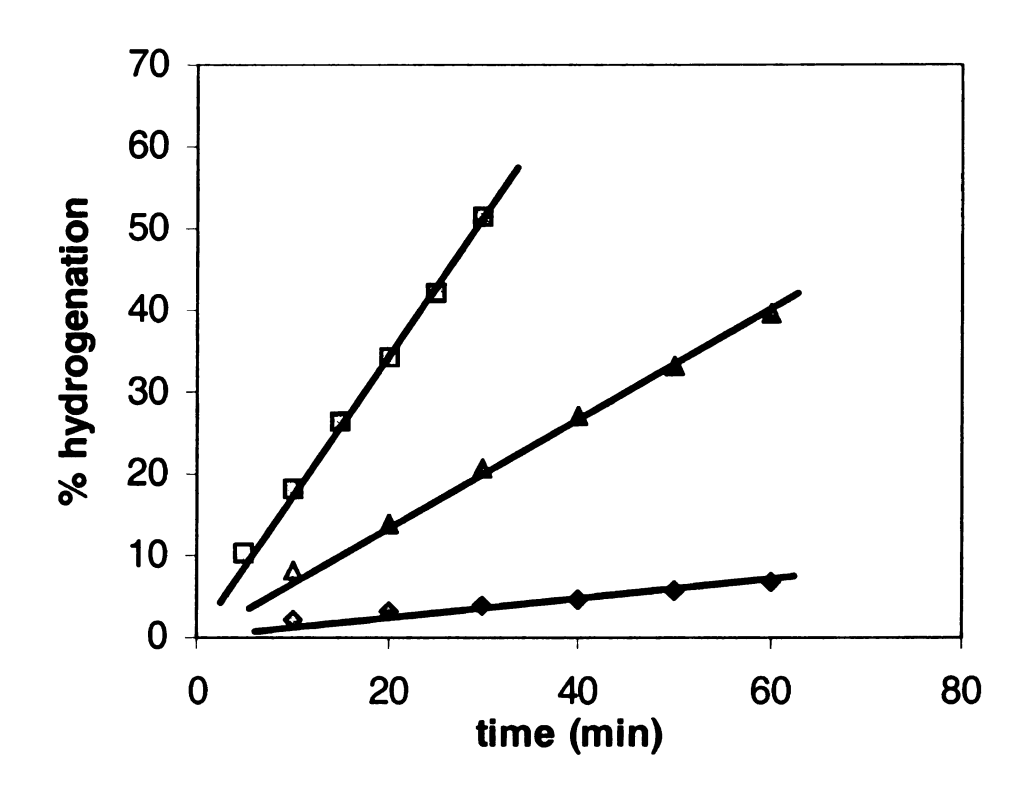


**Figure 2.4.** Percent of substrate hydrogenated *vs* reaction time for allyl alcohol (squares), 1-penten-3-ol (triangles), and 3-methyl-1-penten-3-ol (diamonds) using 3.5-bilayer PAA/PEI-Pd(0)-coated alumina as a catalyst. Percent hydrogenation was obtained from the integration of product and reactant peaks in gas chromatograms.

i r. ii

> pro hyd

th

nan Pd

hyo

subs

In practical applications of selective catalysts, such as minimizing the number of purification steps involved in organic reactions, one substrate must be hydrogenated in the presence of several impurities.<sup>32</sup> In an equimolar mixture of 1 and 2, use of the commercial 5% Pd-on-alumina catalyst results in almost no selectivity between these substrates. However, when using the 3.5-bilayer PAA/PEI-Pd(0)-on-alumina catalyst, the conversion of 2 is only 46% when 1 is 93% converted. Selective conversion is more dramatic for the hydrogenation of a mixture of 1 and 3, where the conversion of 3 is 14% when that of 1 is 91%. However, because the rate of hydrogenation is first-order with respect to the allylic alcohol concentration, the rate of hydrogenation of 1 decreases at high conversions, and thus it may be difficult to achieve 99% conversion of 1 with minimal conversion of other substrates. (In noncompetitive reactions, decreasing the initial concentration of allyl alcohol by a factor of 10 gave a 7-fold decrease in TOF, suggesting a reaction order of 0.85.)

Another important asset of encapsulated nanoparticles is that they may decrease the amount of hydrogenation.<sup>13, 19</sup> Substrate isomerization is a common but unwanted process in hydrogenation, and in some cases, this side reaction is even dominant over hydrogenation.<sup>33</sup> Minimization of isomerization is thus desirable to improve the yield of hydrogenation reactions. Hydrogenation of 1 with polyelectrolyte-encapsulated Pd nanoparticles produces 60% less acetone than does hydrogenation with the commercial Pd catalyst at similar yields. Similar decreases in isomerization were observed with substrate 2.

# 2.3.4. Mechanism of Selective Hydrogenation

To understand the mechanism behind selective hydrogenation by encapsulated nanoparticles, we examined substrate diffusion through an alumina membrane (0.02-µm pore size) coated with seven PAA/PEI bilayers.<sup>34</sup> Figure 2.5 shows that the ratio of the transport rates through the membrane for 1/2 was about 4, and that for 1/3 was 15. The transport experiments suggest that differential rates of transport to the Pd nanoparticles may account for selectivities. First-order reaction rates are also consistent with diffusionlimited kinetics. We hypothesize that both diffusion through PAA/PEI films and access to Pd nanoparticles rely on specific paths through the polyelectrolyte matrix. Larger substrate molecules may have fewer paths available to them, and thus they diffuse more slowly through membranes and to active sites. In addition to size issues, the greater hydrophobicity of the larger alcohols may also limit their access to hydrophilic transport pathways. Coating of the commercial catalyst with 3.5 bilayers of PAA/ PEI resulted in a selectivity of 5 for hydrogenation of 1/3 along with a ~40-fold reduction in the rate of hydrogenation of 1 (Table 1, column 6). These results are consistent with diffusionbased selectivity, but they suggest that there are differences in transport pathways to the commercial catalyst and the embedded nanoparticles.

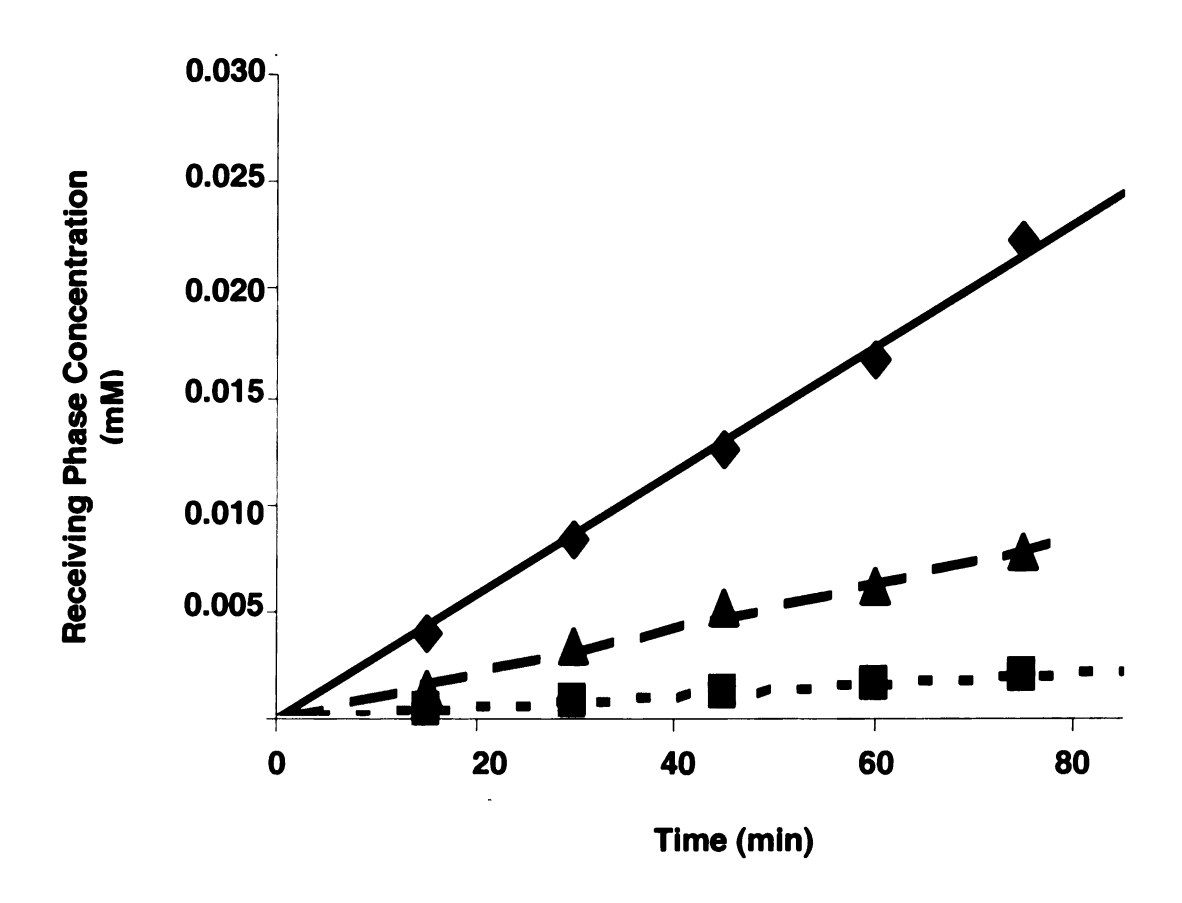


**Figure 2.5**. Receiving phase concentration as a function of time during diffusive transport of substrates through 0.02 μm-alumina membrane coated with (PAA/PEI)<sub>7</sub> film. The substrates were allyl alcohol (squares), 1-penten-3-ol (triangles), and 3-methyl-1-penten-3-ol (diamonds). The source phase contained 20 mM of each substrate in water while the receiving phase initially contained deionized water. Receiving phase concentrations were determined from the integration of substrate peaks in gas chromatograms.

# 2.4. Conclusions

In conclusion, layer-by-layer deposition of PAA and PEI-Pd(II) on alumina and subsequent reduction of Pd<sup>2+</sup> is a versatile method for synthesizing immobilized Pd catalysts. The polyelectrolyte matrix stabilizes the particles, introduces selectivity, and appears to decrease unwanted isomerization. Further exploitation of the versatility of polyelectrolyte films should increase selectivity in hydrogenation as well as other reactions.

# 2.5. References

- 1. Alvarez, M. M.; Khoury, J. T.; Schaaff, T. G.; Shafigullin, M. N.; Vezmar, I.; Whetten, R. L. *Journal of Physical Chemistry B* **1997**, 101, (19), 3706-3712.
- 2. Chen, S.; Ingrma, R. S.; Hostetler, M. J.; Pietron, J. J.; Murray, R. W.; Schaaff, T. G.; Khoury, J. T.; Alvarez, M. M.; Whetten, R. L. Science 1998, 280, (5372), 2098-2101.
- 3. Quinn, B. M.; Liljeroth, P.; Ruiz, V.; Laaksonen, T.; Kontturi, K. *Journal of the American Chemical Society* **2003**, 125, (22), 6644-6645.
- 4. Schmid, G. Nanoscale Materials in Chemistry 2001, 15-59.
- 5. Suzdalev, I. P.; Suzdalev, P. I. Russian Chemical Reviews 2001, 70, (3), 177-210.
- 6. Haruta, M. Chemical Record **2003**, 3, (2), 75-87.
- 7. Schimpf, S.; Lucas, M.; Mohr, C.; Rodemerck, U.; Bruckner, A.; Radnik, J.; Hofmeister, H.; Claus, P. Catalysis Today 2002, 72, (1-2), 63-78.
- 8. Valden, M.; Lai, X.; Goodman, D. W. Science 1998, 281, (5383), 1647-1650.
- 9. Zanella, R.; Louis, C.; Giorgio, S.; Touroude, R. *Journal of Catalysis* **2004**, 223, (2), 328-339.
- 10. Li, Y.; Boone, E.; El-Sayed, M. A. Langmuir **2002**, 18, (12), 4921-4925.
- 11. Rao, C. N. R.; Kulkarni, G. U.; Thomas, P. J.; Edwards, P. P. Chemistry--A European Journal 2002, 8, (1), 28-35.
- 12. Li, Y.; El-Sayed, M. A. Journal of Physical Chemistry B 2001, 105, (37), 8938-8943.
- 13. Niu, Y.; Yeung, L. K.; Crooks, R. M. *Journal of the American Chemical Society* **2001**, 123, (28), 6840-6846.

- 14. Park, J. H.; Lim, Y. T.; Park, O. O.; Kim, J. K.; Yu, J.-W.; Kim, Y. C. Chemistry of Materials 2004, 16, (4), 688-692.
- 15. Lee, J.-E.; Kim, J.-W.; Jun, J.-B.; Ryu, J.-H.; Kang, H.-H.; Oh, S.-G.; Suh, K.-D. Colloid and Polymer Science **2004**, 282, (3), 295-299.
- 16. Ye, J.-S.; Ottova, A.; Tien, H. T.; Sheu, F.-S. *Bioelectrochemistry* **2003**, 59, (1-2), 65-72.
- 17. Fendler, J. H.; Editor, Nanoparticles and Nanostructured Films: Preparation, Characterization and Applications. 1998; p 468 pp.
- 18. Zhao, M.; Sun, L.; Crooks, R. M. Journal of the American Chemical Society **1998**, 120, (19), 4877-4878.
- 19. Crooks, R. M.; Zhao, M.; Sun, L.; Chechik, V.; Yeung, L. K. Accounts of Chemical Research 2001, 34, (3), 181-190.
- 20. Underhill, R. S.; Liu, G. Chemistry of Materials 2000, 12, (12), 3633-3641.
- 21. Decher, G. Science 1997, 277, (5330), 1232-1237.
- 22. Iler, R. K. Journal of Colloid and Interface Science 1966, 21, (6), 569-94.
- 23. Lvov, Y.; Decher, G.; Moehwald, H. Langmuir 1993, 9, (2), 481-6.
- 24. Liu, Y.; Wang, Y.; Claus, R. O. Chemical Physics Letters 1998, 298, (4-6), 315-319.
- 25. Schmitt, J.; Decher, G.; Dressick, W. J.; Brandow, S. L.; Geer, R. E.; Shashidhar, R.; Calvert, J. M. Advanced Materials 1997, 9, (1), 61-65.
- 26. Dai, J.; Bruening, M. L. Nano Letters 2002, 2, (5), 497-501.
- 27. Wang, T. C.; Rubner, M. F.; Cohen, R. E. Langmuir 2002, 18, (8), 3370-3375.

- 28. Miller, M. D.; Bruening, M. L. Chemistry of Materials 2005, 17, (21), 5375-5381.
- 29. Liu, X.; Bruening, M. L. Chemistry of Materials 2004, 16, (2), 351-357.
- 30. Dai, J.; Balachandra, A. M.; Lee, J. I.; Bruening, M. L. *Macromolecules* **2002**, 35, (8), 3164-3170.
- 31. Scott, R. W. J.; Ye, H.; Henriquez, R. R.; Crooks, R. M. Chemistry of Materials **2003**, 15, (20), 3873-3878.
- 32. Cerveny, L.; Ruzicka, V. Catalysis Reviews Science and Engineering 1982, 24, (4), 503-66.
- 33. Zharmagambetova, A. K.; Ergozhin, E. E.; Sheludyakov, Y. L.; Mukhamedzhanova, S. G.; Kurmanbayeva, I. A.; Selenova, B. A.; Utkelov, B. A. *Journal of Molecular Catalysis A: Chemical* **2001**, 177, (1), 165-170.
- 34. Stair, J. L.; Harris, J. J.; Bruening, M. L. Chemistry of Materials 2001, 13, (8), 2641-2648.

# Chapter 3: Pd Nanoparticles Encapsulated in Reduced [PdCl<sub>4</sub><sup>2</sup>/PEI]<sub>n</sub>

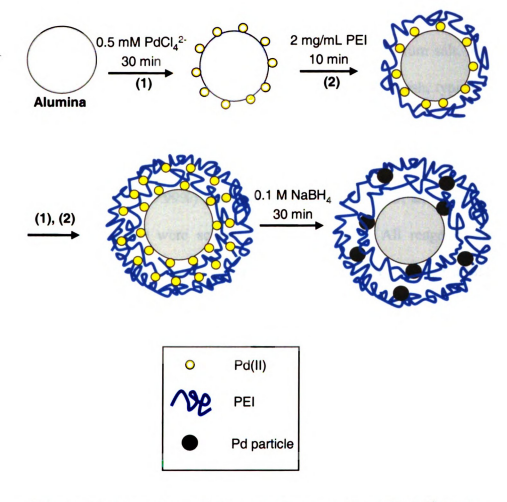
Films: Highly Active Catalysts for Selective Hydrogenation

# 3.1. Introduction

As mentioned in the first two chapters, catalysis provides a natural application for nanoparticles because their large surface area to volume ratio allows effective utilization of expensive metals.<sup>1-3</sup> Without a suitable support, however, metal particles aggregate, reducing surface area and restricting control over particle size. For example, during the selective hydrogenation of citral to citronellal, surfactant-stabilized Ni boride catalysts were employed.<sup>4, 5</sup> In this case, the surfactant molecules could adsorb onto the surface of the nanoparticles, and acted as a protective agent to stabilize and restrict the growth of particles. Encapsulation by polymers is advantageous because in addition to stabilizing and protecting the particles, the encapsulating polymers offer unique possibilities for modifying both the environment around catalytic sites and access to these sites. 6-11 Hence, the protective polymer not only influences particle sizes and morphologies but can also have a tremendous influence on catalytic activity and selectivity. For example, Schmid et al. performed the hydrogenation of 2-hexyne catalyzed by 2-nbutylphenanthroline-protected Pd nanoparticles to give cis-2-hexene as the major product.<sup>12</sup> Typically, Crooks and co-workers have reported that the hydrogenation of allyl alcohol is 11-fold faster than hydrogenation of 3-methyl-1-penten-3-ol when using palladium nanocatalysts incorporated in a dendrimer system.<sup>3</sup> Thus, variation of the matrix around catalytic nanoparticles should help in tuning of catalytic properties while stabilizing these particles.

In the previous chapter, <sup>13</sup> we described selective hydrogenation using Pd nanoparticles embedded in poly(acrylic acid) (PAA)/polyethyleneimine (PEI) films. In this chapter, we further examine the deposition, characterization, and catalytic properties of these films and compare them with a new catalytic system that is prepared by alternating immersions of a substrate in PdCl<sub>4</sub><sup>2-</sup> and PEI solutions followed by reduction of Pd(II) (Scheme 3.1).<sup>14, 15</sup> This procedure builds on work by Watanabe and Regen that showed the deposition of dendrimer/PtCl<sub>4</sub><sup>2-</sup> films, <sup>15</sup> as well as research by Liu et al. that demonstrated formation of Pd nanoparticles on glassy carbon by electrochemical reduction of films prepared by adsorption of PdCl<sub>4</sub><sup>2-</sup> and an electroactive polycation.<sup>14</sup> Relative to Liu's procedure, we use a different polycation and chemical, rather than electrochemical, reduction.

Nanoparticles in both [PAA/PEI-Pd(0)]<sub>n</sub>PAA and reduced [PdCl<sub>4</sub><sup>2</sup>-/PEI]<sub>n</sub> films can catalyze hydrogenation of allyl alcohol at a rate that is an order of magnitude faster than hydrogenation of 3-methyl-1-penten-3-ol. However, the catalytic activities of the two systems as a function of the number of bilayers in the film are very different. The turnover frequency of [PAA/PEI-Pd(0)]<sub>n</sub>PAA films decreases with an increasing number of bilayers, while the reduced [PdCl<sub>4</sub><sup>2</sup>-/PEI]<sub>n</sub> system shows the opposite trend. Hence, the reduced [PdCl<sub>4</sub><sup>2</sup>-/PEI]<sub>n</sub> system allows a significantly higher activity per g of catalyst (including the support) for multilayer films. This is likely due to greater accessibility of embedded particles in reduced PdCl<sub>4</sub><sup>2</sup>-/PEI films.



Scheme 3.1. Formation of Pd nanoparticles in reduced  $[PdCl_4^{\ 2'}/PEI]_n$  films.

# 3.2. Experimental Section

# 3.2.1. Materials

Polyethyleneimine (PEI) (Mw = 25~000~Da), poly(acrylic acid) (PAA) (25 wt % in water,  $M_w = 90~000~Da$ ), poly(styrene sulfonate) (PSS) (sodium salt,  $M_w = 125~000~Da$ ), palladium (5 wt % on alumina powder),  $\alpha$ -alumina (100 mesh, typical particle size 75-100  $\mu$ m), allyl alcohol (99%), 1-penten-3-ol (99%), 3-methyl-1-penten-3-ol (99%), and 3,4-dihydroxy-1-butene (99%) were purchased from Aldrich. Potassium tetrachloropalladate(II) (99.99%) was obtained from Alfa Aesar, and potassium chloride and sodium borohydride were acquired from Spectrum. All reagents were used as received, and solutions were prepared with deionized water (Milli-Q, 18.2 M $\Omega$  cm).

# 3.2.2. Preparation of Pd Nanoparticles Encapsulated in Polyelectrolyte Multilayer Films

Synthesis of [PAA/PEI-Pd(0)]<sub>n</sub>PAA films occurred as described in the previous chapter<sup>13</sup>. Briefly, alternating immersion of alumina in solutions of PAA (20mM, pH adjusted to 4.0) and a PEI-Pd(II) complex (1 mg/mL PEI, 2mM K<sub>2</sub>PdCl<sub>4</sub>, pH adjusted to 9.0), followed by reduction of Pd(II) by NaBH<sub>4</sub> yielded catalytic Pd nanoparticles in a PAA/PEI film (Scheme 2.1, Chapter 2). Films were always capped with PAA and rinsed between the depositions of each polyelectrolyte.

In a new method, we synthesized encapsulated Pd nanoparticles using alternating deposition of  $PdCl_4^{2-}$  and PEI on alumina particles and subsequent reduction of Pd(II) as depicted in scheme 3.1.<sup>14</sup> Specifically, 15 g of  $\alpha$ -alumina was mixed with 100 mL of a solution containing 0.5 mM  $PdCl_4^{2-}$  and 0.1 M KCl, and the suspension was stirred

vigorously for 30 min. Subsequently, the alumina was allowed to settle, and the supernatant was decanted. The alumina particles were then washed with three 100-mL aliquots of deionized water to remove excess PdCl<sub>4</sub><sup>2</sup>. To deposit a PEI layer, 100 mL of a PEI solution (2 mg/mL, pH adjusted to 9.0 with 1 M HCl) was added to the Pd(II)-coated alumina, and the particles were stirred for 10 min and washed as described above. Subsequent bilayers were deposited similarly. Reduction of Pd(II) in these films was effected by exposure of the coated alumina to 100 mL of fresh 0.1 M NaBH<sub>4</sub> for 30 min (with stirring). The reduced films were washed three times with water after exposure to NaBH<sub>4</sub>. (Scheme 3.1)

In some cases, alumina was first coated with PSS/PEI and then capped with PdCl<sub>4</sub><sup>2</sup>-/PEI bilayers. The PdCl<sub>4</sub><sup>2</sup>-/PEI was formed as described above, and the PSS/PEI precursor bilayers were deposited in a similar manner using a 10-min exposure to a PSS solution (20 mM PSS, 0.5 M MnCl<sub>2</sub>, pH adjusted to 2.1) instead of PdCl<sub>4</sub><sup>2</sup>. All the catalysts were vacuum dried after NaBH<sub>4</sub> reduction, and no flocculation of the alumina was observed during deposition and rinsing. The coated alumina easily dispersed upon exposure to hydrogenation solutions.

# 3.2.3. Characterization of Pd Nanoparticles

Films ([PdCl<sub>4</sub><sup>2</sup>/PEI]<sub>3</sub>) were deposited on carbon-coated copper grids for transmission electron microscopy (TEM). Prior to film deposition, the grids were cleaned in a UV/ozone cleaner for 1 min, and TEM was performed on a JEOL 100CX microscope using an accelerating voltage of 100 kV. The digital images were taken with a Mega View III Soft Imaging System. Films were prepared using alternating 15-min immersions in 0.5 mM PdCl<sub>4</sub><sup>2-</sup>, 0.1 M KCl, and 5-min immersions in 2 mg/mL PEI with 1-min water rinses between the two depositions. Nanoparticles formed upon reduction with 0.1 M NaBH4 for 15 min. We used somewhat shorter deposition times than those employed for the catalyst synthesis because of the small surface area of the TEM grid.

UV-Visible absorption spectra of [PEI/PdCl<sub>4</sub><sup>2</sup>-]<sub>n</sub> films on quartz slides were obtained using a Perkin-Elmer UV/Vis (model Lambda 40) spectrophotometer. To form films on quartz, slides were alternatively immersed into PEI and PdCl<sub>4</sub><sup>2</sup>- solutions for 10 and 30 min, respectively, with a 1-min water rinse after each deposition. These depositions began with PEI rather than PdCl<sub>4</sub><sup>2</sup>- because quartz is negatively charged at the pH values used in deposition.

X-ray photoelectron spectroscopy (XPS) measurements were performed on coated alumina using a Physical Electronics PHI 5400 ESCA workstation. Ellipsometric thicknesses of films on gold-coated wafers (200 nm of Au sputtered on 20 nm of Cr on Si(100)) were determined using a rotating analyzer ellipsometer (model M-44, J. A. Woollam), assuming a film refractive index of 1.5.

# 3.2.4. Transport Studies.

Diffusion dialysis studies were performed using a home-built dialysis apparatus in which a porous alumina membrane (Whatman Anodisc, 0.02 µm surface pores) coated with either [PdCl<sub>4</sub><sup>2</sup>/PEI]<sub>10</sub> or [PAA/PEI]<sub>7</sub> films was sandwiched between two glass cells.<sup>30</sup> More layers were used in these studies than in catalysis in order to cover the pores in the underlying alumina support. The source cell was filled with 90 mL of a 20 mM solution of the desired unsaturated alcohol (allyl alcohol, 1-penten-3-ol, 3-methyl-1-penten-3-ol, or 3,4-dihydroxy-1-butene), while the receiving cell initially contained 90 mL of deionized water. Both the source and the receiving sides were stirred vigorously to minimize concentration polarization at the membrane interface, and samples of the receiving phase were taken every 15 min and analyzed by gas chromatography (Shimadzu GC-17A equipped with an RTx-BAC1 column).

### 3.2.5. Hydrogenation Reactions

Catalytic hydrogenations were run in a 200-mL, three-neck, round-bottomed flask. H<sub>2</sub> at a gauge pressure of 50 kPa was bubbled through a frit at the bottom of a solution that was vigorously stirred throughout the reaction. Suspensions of catalyst (250 mg) in H<sub>2</sub>O (100 mL) were bubbled with H<sub>2</sub> for 30 min before adding 2.0 mmol of substrate in 100 mL of water. Gas chromatography was used to analyze aliquots of the reaction mixture periodically. The sensitivity of the flame-ionization detector was assumed to be the same for products and reactants because they contain the same number of carbon atoms. (A spot check with allyl alcohol and 1-propanol showed this to be a

good assumption.) GC-MS was used to identify compounds in reactions with multiple products.

# 3.2.6. Determination of the Amount of Pd in Catalysts and Deposition Solutions

Calculation of turnover frequencies (TOFs), i.e., the moles of substrate that are hydrogenated per mole of Pd per hour, requires knowledge of the amount of Pd in the catalyst. To determine Pd content, we employed atomic emission spectroscopy (Varian Spectra AA-200). Standard solutions (0.1 to 0.5 mM) were prepared by dissolving K<sub>2</sub>PdCl<sub>4</sub> in 0.1 M HNO3, and sample solutions were prepared by stirring 250 mg of dried, synthesized catalyst in 2 mL of *aqua regia* for 15 min. These sample solutions were diluted to 12 mL with 0.1 M HNO3 and centrifuged (the α-alumina support does not dissolve in *aqua regia*), and the supernatant was analyzed using its emission at 363.5 nm. When analyzing deposition solutions containing K<sub>2</sub>PdCl<sub>4</sub> in 0.1 M KCl, samples were diluted by a factor of 10, and standards were prepared in 0.01 M KCl rather than 0.1 M HNO<sub>3</sub> to account for interferences from KCl.

# 3.3. Results and Discussion

# 3.3.1. Film Deposition

In investigation of catalysis by nanoparticle-containing films, it is necessary to analyze the film growth and composition. We performed UV/Vis spectroscopy of [PEI/PdCl<sub>4</sub><sup>2-</sup>]<sub>n</sub> films on quartz to demonstrate that layer-by-layer deposition occurs. As shown in Figure 3.1, the absorbance of PEI/PdCl<sub>4</sub><sup>2-</sup> films at 220 nm, which is likely due to a Pd(II)-amine charge transfer band,<sup>3, 16</sup> increases linearly with the number of bilayers. A linear increase in an absorbance peak at 222 nm also occurs with [PEI-Pd(II)/PAA]<sub>n</sub>

(see Figure 2.1, chapter 2), so UV/VIS spectra confirm the layer-by-layer growth of both [PEI/PdCl<sub>4</sub><sup>2-</sup>]<sub>n</sub> and [PEI-Pd(II)/PAA]<sub>n</sub> films.

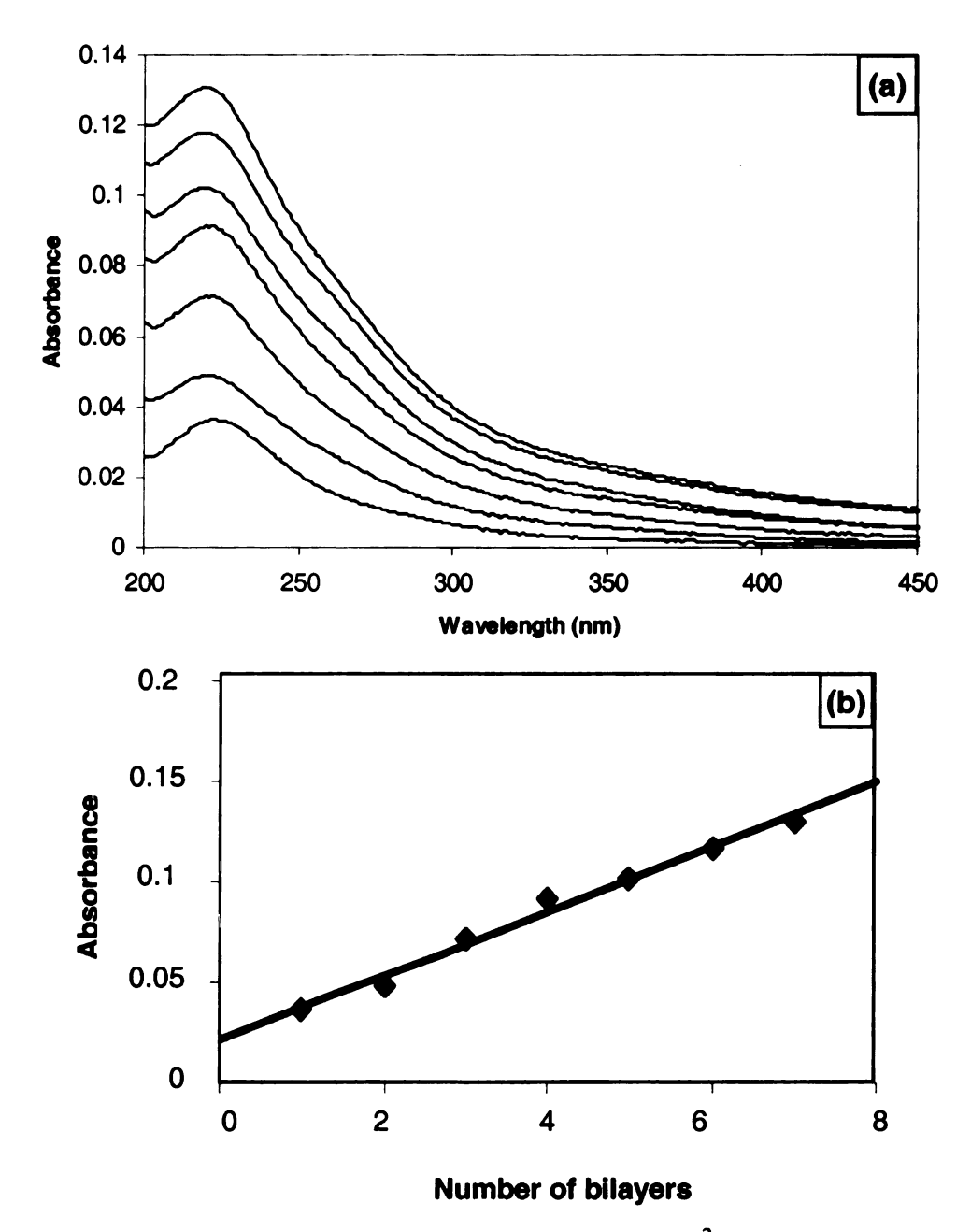
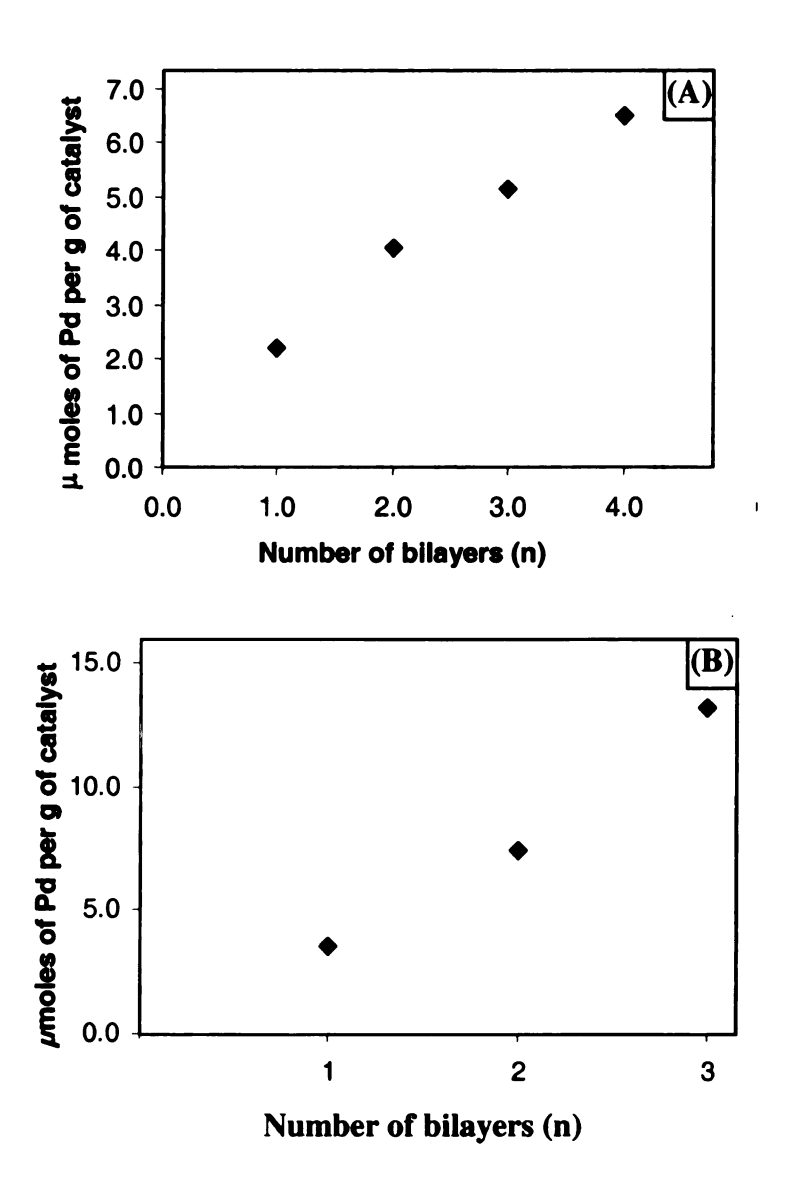


Figure 3.1. UV-Visible absorption spectra of  $[PEI/PdCl_4^{2-}]_n$  films on a quartz substrate with n = 1 to 7 (from lower to upper curves), (a). (b) shows the absorbance at  $\lambda_{max}$  (220 nm) as a function of number of bilayers.

XPS spectra of PEI/PdCl<sub>4</sub><sup>2</sup> films show Cl to Pd ratios less than 1, so we think that Pd in these films is actually bound to PEI, and films are held together by metal-ion coordination. (Thus the nomenclature PEI/PdCl<sub>4</sub><sup>2</sup> reflects deposition conditions and not the state of Pd in the films.)

To verify film growth on alumina particles, we performed atomic emission analysis of Pd. Figure 3.2A shows that the amount of Pd in [PdCl<sub>4</sub><sup>2</sup>/PEI]<sub>n</sub> films increases linearly with the number of bilayers after deposition of the first layer, and similar results occur with [PAA/PEI-Pd(II)]<sub>n</sub>PAA (Figure 3.2B). We also analyzed the solutions employed in the deposition process to determine whether Pd was removed from films during rinsing, reduction, or deposition of PAA ([PAA/PEI-Pd(II)]<sub>n</sub>PAA films) or PEI ([PdCl<sub>4</sub><sup>2</sup>-/PEI]<sub>n</sub> films). On average, less than 10% of the amount of Pd deposited in the most recent step was leached from the catalyst during each deposition of PAA or PEI. Rinsing also leached very little Pd, but reduction with NaBH<sub>4</sub> removed about 15% of the total Pd in [PAA/PEI-Pd]<sub>n</sub>PAA coatings and 60% of the Pd in [PdCl<sub>4</sub><sup>2</sup>-/PEI]<sub>n</sub> films. Electrostatic interactions between PAA and PEI likely ionically cross-link [PAA/PEI-Pd]PAA films and help prevent removal of Pd. Another important point from atomic emission results is that because of the high surface area of the alumina, deposition solutions do lose around 60% of their Pd during adsorption. Thus, we used fresh solutions for each deposition step.

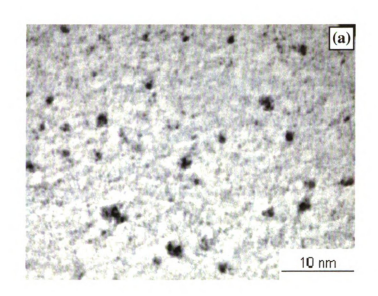


**Figure 3.2.** (A) Micromoles of Pd (determined by atomic emission spectroscopy) per g of catalyst for several values of n in [PdCl<sub>4</sub><sup>2-</sup>/PEI]<sub>n</sub> films deposited on alumina. (Analysis was performed after reduction of the Pd(II) with NaBH<sub>4</sub> as described in the text.) (B) The corresponding plot for [PAA/PEI-Pd(0)]<sub>n</sub>PAA films on alumina.

#### 3.3.2. Film Characterization

To investigate the reduction of Pd(II) to form nanoparticles, we performed both TEM and XPS. The TEM image in Figure 3.3 confirms the formation of Pd nanoparticles during exposure of [PdCl<sub>4</sub><sup>2</sup>·/PEI]<sub>3</sub> films to NaBH<sub>4</sub>. The particles have diameters of 1 to 4 nm and are distributed throughout the film. (We note that there may be particles with diameters <1 nm, but these would be difficult to see and likely unstable. Figure 3.3 also shows a histogram of particle sizes > 1 nm.) In the previous chapter, PAA/PEI-Pd(0) films showed a similar distribution of nanoparticles with sizes ranging from 1 to 3 nm.<sup>13, 18</sup> The ellipsometric thicknesses of [PEI/PAA]<sub>3</sub>PEI and [PEI/PdCl<sub>4</sub><sup>2-</sup>]<sub>3</sub> films on gold-coated Si wafers were 125 Å and 65 Å, respectively. Thicknesses on the carbon-coated Cu grid should be similar, so TEM images should probe the entire depth of the film.

XPS provides information about the Pd oxidation state in reduced PdCl<sub>4</sub><sup>2</sup>/PEI and PAA/PEI-Pd(0) films because photoelectrons with energies of 337 and 342 eV correspond to Pd(II), while those at 335 and 340 eV correspond to Pd(0).<sup>19</sup> Figure 3.4 contains the XPS spectra of [PAA/PEI-Pd(0)]<sub>3</sub>PAA and [PdCl<sub>4</sub><sup>2</sup>/PEI]<sub>3</sub> films on alumina before and after reduction with NaBH<sub>4</sub>. These spectra indicate that approximately 70% of the Pd in these films is reduced from Pd(II) to Pd(0) upon exposure to NaBH<sub>4</sub>. The incomplete reduction could arise due to inaccessibility of a few Pd ions to NaBH<sub>4</sub> or air oxidation of a small amount of Pd(0).<sup>16</sup> (Given the thicknesses of these films and a sampling depth in XPS of about 100 Å, most of the film is being probed in these measurements. However, XPS is not capable of probing films adsorbed in the alumina pores).



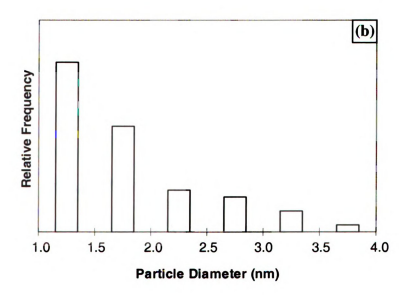


Figure 3.3 (a) TEM image of a [PdCl<sub>4</sub><sup>2</sup>/PEI]<sub>3</sub> film deposited on a carbon-coated copper grid and reduced with NaBH<sub>4</sub> and (b) the histogram of particle sizes obtained from the above TEM image.

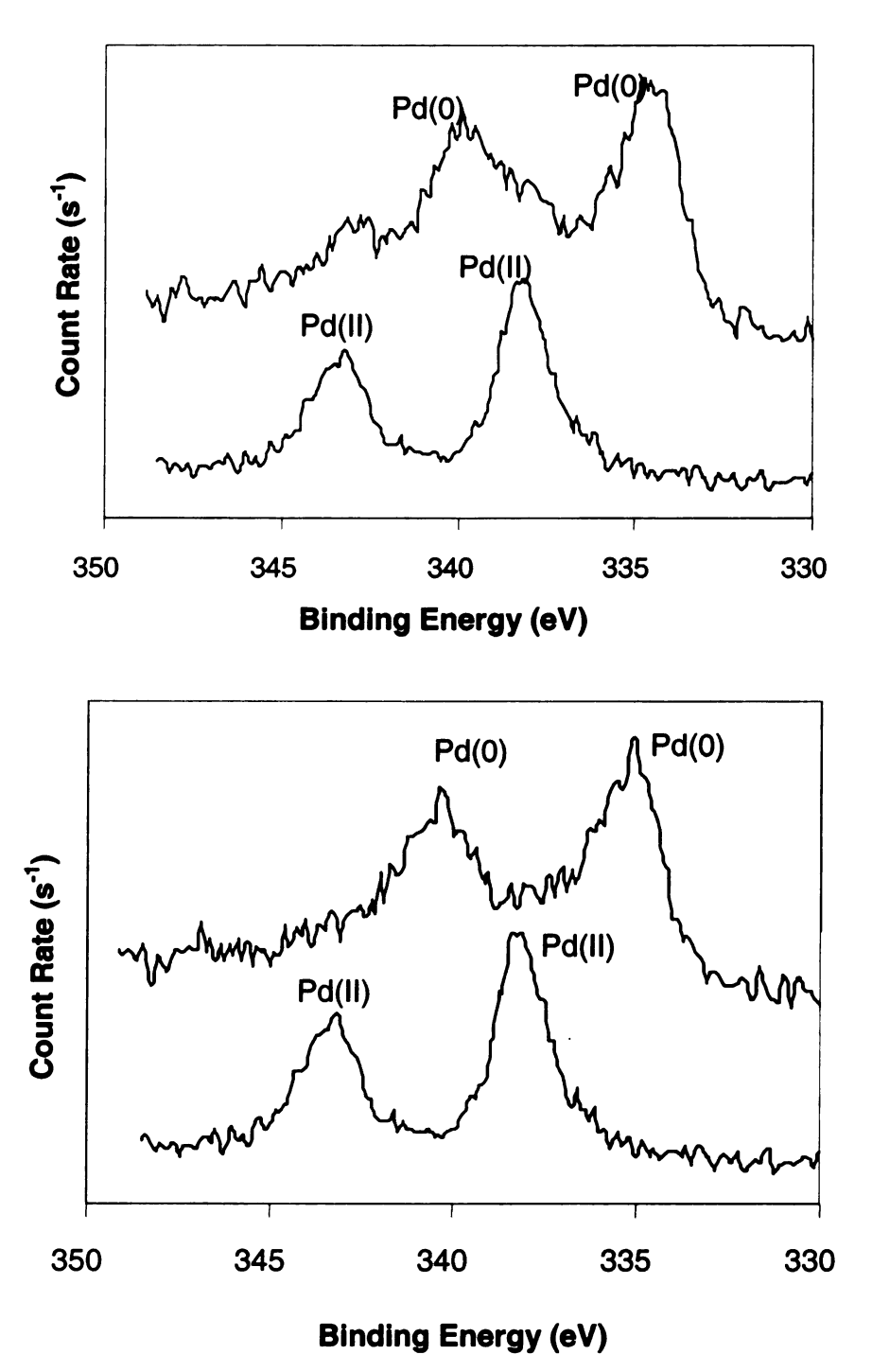


Figure 3.4. (a) XPS spectra of a [PAA/PEI-Pd]<sub>3</sub>PAA film on alumina before (bottom) and after (top) reduction with NaBH<sub>4</sub>. (b) Corresponding spectra of [PdCl<sub>4</sub><sup>2</sup>-/PEI]<sub>3</sub> films on alumina.

#### 3.3.3. Catalysis of Hydrogenation

To investigate some of the catalytic properties of reduced Pd in polyelectrolyte films, we hydrogenated a series of unsaturated alcohols using the nanoparticles as catalysts. We studied hydrogenation rates as a function of substrate concentration and film composition to probe catalytic activity as well as film structure.

#### 3.3.3.1. Reaction Kinetics.

Figure 3.5 demonstrates how the rate of allyl alcohol hydrogenation catalyzed by reduced [PdCl<sub>4</sub><sup>2</sup>/PEI]<sub>3</sub> on alumina varies with initial allyl alcohol concentration. Increasing the concentration of allyl alcohol by a factor of 10 gives on average a 9-fold increase in TOF, implying a reaction order of ~1. Similar kinetics (approximately first order) were observed with the PAA/PEI-Pd(0) system.<sup>13, 18</sup> In reactions with conventional Pd catalysts, hydrogenation is typically zero order with respect to substrate concentration, probably because the Pd in such catalysts is saturated with substrate.<sup>20, 21</sup> In contrast, for nanoparticles in polyelectrolyte multilayers, the first-order kinetics suggest that the rate-limiting step involves either diffusion of the substrate to the nanoparticles or slow adsorption. Selectivities among substrates and the transport studies discussed below indicate that diffusion may be the rate-limiting process in these reactions.

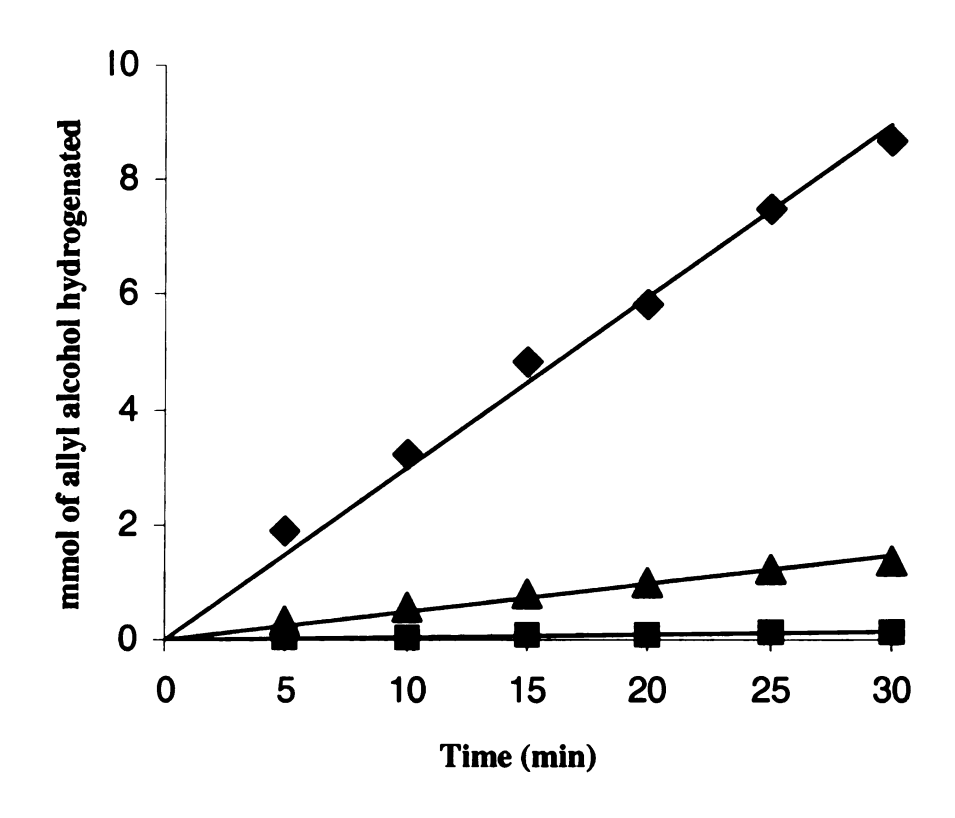


**Figure 3.5.** Amount of allyl alcohol hydrogenated *vs* reaction time for 200-mL solutions initially containing 20 mmol (diamonds), 2 mmol (triangles), and 0.2 mmol (squares) of allyl alcohol. The catalyst was 250 mg of alumina coated with a reduced [PdCl<sub>4</sub><sup>2</sup>-/PEI]<sub>3</sub> film.

# 3.3.3.2. Catalytic Activity of Reduced [PdCl<sub>4</sub><sup>2</sup>-/PEI]<sub>n</sub> as a Function of the Substrate and Film Composition.

Table 3.1 summarizes the TOFs for catalysis of hydrogenation of several substrates by reduced  $[PdCl_4^2/PEI]_n$  films. The substrates for hydrogenation, allyl alcohol (1), 1-penten-3-ol (2), and 3-methyl-1-penten-3-ol (3), differ only in the substituents at the  $\alpha$ -carbon of the double bond, but with reduced  $[PdCl_4^2/PEI]_4$  films as catalysts, hydrogenation rates for 1 are 11-fold higher than those for 3. For alumina coated with only reduced  $PdCl_4^2$  (n=0.5), TOFs are very high, but reaction rates for the different substrates vary by a factor of less than 1.4. This shows that the presence of additional alkyl groups at the  $\alpha$ -carbon does not significantly alter reactivity. Thus, the selectivity of hydrogenation using reduced  $PdCl_4^2/PEI$  films does not stem from differences in the electronic properties of the substrates.

With a commercially available 5%-Pd-on-alumina catalyst (Aldrich), hydrogenation rates for the three unsaturated alcohols are also very close (1/2≈1/3=0.87). However, TOFs are 4-fold lower for the commercial catalyst than for the reduced PdCl<sub>4</sub><sup>2-</sup> (n=0.5) system. The high activity of reduced PdCl<sub>4</sub><sup>2-</sup> on alumina may result from small Pd nanoparticles with a large surface area, but we should note that the Pd loading in these catalysts is only 0.034 wt%. Hence, rates of hydrogenation per g of catalyst (including the support) are still ~40-fold higher with the commercial 5%-Pd-on-alumina.

**Table 3.1**. TOFs (moles hydrogenated per mol Pd per h) for hydrogenation of allylic alcohols using several catalysts

		5%	Reduced [PdCl <sub>4</sub> <sup>2</sup> /PEI] <sub>n</sub> catalysts on alumina for several values of n <sup>b</sup>					
		Pd/Al <sub>2</sub> O <sub>3</sub> <sup>a</sup>	$n = 0.5^{c}$	n = 1	n = 2	n = 3	n = 4	$1.0 + 2.0^{d}$
1	OH	1300±150	5880/6130	820/670	750/1100	1990/1670	1220/1630	720/750
2	OH	1500±120	5570/5940	230/190	240/440	690/530	450/540	250/280
3	OH	1500±100	4250/4720	190/140	110/150	260/170	110/150	50/70

<sup>a</sup>TOF values for commercially available 5%-Pd-on-alumina catalyst are from ref. 13

<sup>b</sup>Values are given for replications of the same reaction with two different batches of catalyst. Small, random differences in the film formation processes may account for the variations in TOFs for the same system. The hydrogenation solution originally contained 2.0 mmol of unsaturated alcohol in 200 ml of water, and the TOF represents the initial rate.

'This film was prepared by adsorption of only PdCl<sub>4</sub><sup>2</sup> and subsequent reduction with NaBH<sub>4</sub>.

<sup>d</sup>[PSS/PEI]<sub>1</sub>/[PdCl<sub>4</sub><sup>2</sup>-/PEI]<sub>2</sub>.

Relative to the reduced PdCl<sub>4</sub><sup>2</sup> (n=0.5) catalyst, the presence of a PEI layer in a reduced [PdCl<sub>4</sub><sup>2</sup>/PEI]<sub>1</sub> system decreases the TOF for allyl alcohol by a factor of ~8. The decrease in TOF is more appreciable for 2 and 3, resulting in 1/2 and 1/3 average selectivities of 3.5 and 4.6, respectively. The decrease in rates after PEI adsorption could occur in part because Pd nanoparticles that are present in the alumina pores become inaccessible after coating with a layer of PEI. In addition, the PEI likely provides selectivity by controlling the rate of transport to accessible nanoparticles. The possible presence of inaccessible Pd in alumina pores might explain why the TOF for allyl alcohol increases on going from [PdCl<sub>4</sub><sup>2</sup>-/PEI]<sub>1</sub> to [PdCl<sub>4</sub><sup>2</sup>-/PEI]<sub>3</sub> or [PdCl<sub>4</sub><sup>2</sup>-/PEI]<sub>4</sub> catalysts. Inaccessible Pd would decrease the TOF for all of the films, but the fraction of Pd that is in the alumina pores should be less for thicker films. Because the initial bilayer contains nearly 2-fold more Pd than the 3<sup>rd</sup> and 4<sup>th</sup> bilayers (see Figure 3.2 A), the effect of inaccessible Pd could be significant. Eventually, however, decreases in TOFs due to longer transport pathways to underlying layers should overcome the fact that the fraction of Pd that is inaccessible in support pores decreases with an increasing number of bilayers.

In an effort to understand whether inactive Pd nanoparticles in the support decrease the activity of the catalyst, we examined catalysis by reduced [PSS/PEI]<sub>1</sub>/[PdCl<sub>4</sub><sup>2</sup>-/PEI]<sub>2</sub> coatings. We thought that these films would have a higher TOF after reduction than reduced [PdCl<sub>4</sub><sup>2</sup>-/PEI]<sub>2</sub> films, since the initial bilayer of PSS/PEI could cover the pores of alumina (at least partially) and decrease deposition of inaccessible Pd. However, TOFs of reduced [PSS/PEI]<sub>1</sub>/[PdCl<sub>4</sub><sup>2</sup>-/PEI]<sub>2</sub> films are about the same or slightly lower than those of reduced [PdCl<sub>4</sub><sup>2</sup>-/PEI]<sub>2</sub> films (Table 3.1). With

reduced [PSS/PEI]<sub>4</sub>/[PdCl<sub>4</sub><sup>2</sup>-/PEI]<sub>2</sub> films, TOF decreased even further (TOF of 330 for allyl alcohol). Decreases in TOF could occur because of penetration of Pd into the precursor layer,<sup>22</sup> which also might explain the increased deposition of Pd in [PSS/PEI]<sub>1</sub>/[PdCl<sub>4</sub><sup>2</sup>-/PEI]<sub>2</sub> and [PSS/PEI]<sub>4</sub>/[PdCl<sub>4</sub><sup>2</sup>-/PEI]<sub>2</sub> films (1.4 x 10<sup>-6</sup> moles in 250 mg of catalyst for both systems) relative to [PdCl<sub>4</sub><sup>2</sup>-/PEI]<sub>2</sub> films (1.0 x 10<sup>-6</sup> moles in 250 mg). Another explanation for the lower turnover frequency in reduced [PSS/PEI]<sub>1</sub>/[PdCl<sub>4</sub><sup>2</sup>-/PEI]<sub>2</sub> and [PSS/PEI]<sub>4</sub>/[PdCl<sub>4</sub><sup>2</sup>-/PEI]<sub>2</sub> films might be the intermingling of PSS in PdCl<sub>4</sub><sup>2</sup>-/PEI layers,<sup>23</sup> which would likely yield a more ionically cross-linked, less permeable film.

# 3.3.3.3. Catalytic Activity of Reduced [PAA/PEI-Pd(0)]<sub>n</sub>PAA as a Function of the Substrate and Film Composition.

We thought that the catalytic activity of Pd in [PAA/PEI-Pd(0)]<sub>n</sub>PAA would be lower than in reduced PdCl<sub>4</sub><sup>2</sup>/PEI because the PAA should help to restrict access to Pd nanoparticles. Table 3.2 shows that TOFs of [PAA/PEI-Pd(0)]<sub>3</sub>PAA films are indeed about half of those for reduced [PdCl<sub>4</sub><sup>2</sup>-/PEI]<sub>3</sub> and [PdCl<sub>4</sub><sup>2</sup>-/PEI]<sub>4</sub> films. However, unlike the [PdCl<sub>4</sub><sup>2</sup>-/PEI]<sub>n</sub> system, the TOFs of [PAA/PEI-Pd(0)]<sub>n</sub>PAA films decrease with an increasing number of bilayers. This decrease in TOF reflects an approximately linear increase in Pd content with an increasing number of bilayers (see Figure 3.2 B) along with a relatively constant reaction rate. The initial deposition of PAA and the binding of Pd to PEI should minimize deposition of Pd in alumina pores in this system. Thus, the regular decrease in turnover frequency with the addition of more bilayers most likely shows that with [PAA/PEI-Pd(0)]<sub>n</sub>PAA, the hydrogenation reaction is effected primarily by Pd nanoparticles present in the outer-most layer of the catalyst. Ionic cross-linking in

[PAA/PEI-Pd(0)]<sub>n</sub>PAA films likely restricts access to inner portions of the film. In contrast, reduced [PdCl<sub>4</sub><sup>2</sup>/PEI]<sub>n</sub> coatings probably allow catalysis throughout the film, and thus this multilayered system gives a significantly higher activity per g of catalyst (including the support).

## 3.3.4. Roles of Size and Polarity in Selectivity

The molecules listed in Tables 3.1 and 3.2 differ in size, but they also differ in polarity. To investigate whether selectivities are due primarily to polarity or size effects, we examined hydrogenation of 3,4-dihydroxy-1-butene (4). Table 3.3 shows the TOFs for hydrogenation of 1-4 using alumina coated with reduced [PdCl<sub>4</sub><sup>2</sup>/PEI]<sub>3</sub> films. Even though 4 is more polar than 2, the TOFs of these two substrates are within 30% of each other, suggesting that size is the primary factor controlling the rate of hydrogenation.

**Table 3.2**. Hydrogenation TOFs for catalysts containing  $[PAA/PEI-Pd(0)]_nPAA$  films on alumina with several values of n.

		n = 1 <sup>a</sup>	n = 2 <sup>a</sup>	n = 3 <sup>b</sup>
1	OH	2130/2150	1260/1170	730±130
2	OH	810/970	370/380	280±20
3	ОН	280/350	130/120	60±15

<sup>&</sup>lt;sup>a</sup>Values are given for replications of the same reaction with two different batches of catalyst. The hydrogenation solution originally contained 2.0 mmol of unsaturated alcohol in 200 ml of water, and the TOF represents the initial rate.

Table 3.3. Hydrogenation TOFs for reduced [PdCl<sub>4</sub>-2/PEI]<sub>3</sub> films on alumina

		TOFª
1	OH	1990/1670
2	OH	690/530
3	OH	260/170
4	ОН	940/740

<sup>a</sup>Values are given for replications of the same reaction with two different batches of catalyst. The hydrogenation solution originally contained 2.0 mmol of unsaturated alcohol in 200 ml of water, and the TOF represents the initial rate.

<sup>&</sup>lt;sup>b</sup>TOF values from ref. 13

#### 3.3.5. Transport Studies.

To better understand the mechanism behind selective hydrogenation by encapsulated nanoparticles, we examined substrate diffusion through a porous alumina membrane (0.02-\mu m pore size) coated with unreduced [PdCl<sub>4</sub><sup>2</sup>/PEI]<sub>10</sub> films. The ratios of transport rates for 1/2, 1/4, and 1/3 were about 1.7, 2.0, and 3.1, respectively. Transport studies performed with reduced [PdCl<sub>4</sub><sup>2</sup>-/PEI]<sub>7</sub> films on porous alumina showed selectivities similar to those of the non-reduced films. The transport experiments suggest that differential rates of diffusion to the Pd nanoparticles could play a role in selective catalysis, but the diffusion dialysis selectivities are 3- to 4-fold lower than catalytic selectivities of reduced [PdCl<sub>4</sub><sup>2</sup>-/PEI]<sub>4</sub>. We surmise that both diffusion through [PdCl<sub>4</sub><sup>2</sup>-/PEI]<sub>n</sub> films and access to Pd nanoparticles rely on specific paths through the polyelectrolyte matrix. Selective diffusion of substrates to active sites on nanoparticles may not be completely reflected in diffusion dialysis, because transport through a [PdCl<sub>4</sub><sup>2</sup>/PEI]<sub>n</sub> membrane could bypass embedded particles. In the case of PAA/PEI-Pd, diffusion studies through an alumina membrane coated with a [PAA/PEI]<sub>7</sub> film were reported in chapter 2.<sup>13</sup> The ratios of the transport rates through such membranes are about 4 for 1/2 and 15 for 1/3. In this system, catalytic selectivities are quite similar to transport selectivities, suggesting that diffusion does control reaction rates.

#### 3.4. Conclusions

Deposition of Pd(II) in polyelectrolyte films followed by reduction yields catalytic, nanoparticle-containing films, and such films can serve as selective catalysts in the hydrogenation of small, unsaturated alcohols. For [PAA/PEI-Pd(0)]<sub>n</sub>PAA films,

TOFs decrease with the number of bilayers, suggesting that mainly the outer layers of the film effect catalysis. However, TOFs for reduced  $[PdCl_4^2/PEI]_n$  films show the opposite trend, demonstrating that there are structural differences between these two catalytic systems. Transport studies and reaction orders suggest that catalytic selectivities are due to selective diffusion of the reactant molecules to catalytic sites, and selective access is primarily a function of substrate size, not polarity.

#### 3.5. References

- 1. Fendler, J. H.; Editor, Nanoparticles and Nanostructured Films: Preparation, Characterization and Applications. 1998; p 468 pp.
- 2. Li, Y.; Boone, E.; El-Sayed, M. A. Langmuir 2002, 18, (12), 4921-4925.
- 3. Niu, Y.; Yeung, L. K.; Crooks, R. M. Journal of the American Chemical Society **2001**, 123, (28), 6840-6846.
- 4. Chiang, S.-J.; Liaw, B.-J.; Chen, Y.-Z. Applied Catalysis, A: General 2007, 319, 144-152.
- 5. Liaw, B.-J.; Chiang, S.-J.; Tsai, C.-H.; Chen, Y.-Z. Applied Catalysis, A: General **2005**, 284, (1-2), 239-246.
- 6. Bonnemann, H.; Richards, R. M. European Journal of Inorganic Chemistry 2001, (10), 2455-2480.
- 7. Ciebien, J. F.; Cohen, R. E.; Duran, A. Supramolecular Science 1998, 5, (1-2), 31-39.
- 8. Ciebien, J. F.; Cohen, R. E.; Duran, A. Materials Science & Engineering, C: Biomimetic and Supramolecular Systems 1999, C7, (1), 45-50.
- 9. Dante, S.; Advincula, R.; Frank, C. W.; Stroeve, P. *Langmuir* **1999**, 15, (1), 193-201.
- 10. Kralik, M.; Biffis, A. Journal of Molecular Catalysis A: Chemical 2001, 177, (1), 113-138.
- 11. Mayer, A. B. R.; Mark, J. E. Journal of Polymer Science, Part A: Polymer Chemistry 1997, 35, (15), 3151-3160.
- 12. Schmid, G.; Maihack, V.; Lantermann, F.; Peschel, S. Journal of the Chemical Society, Dalton Transactions: Inorganic Chemistry 1996, (5), 589-95.

- 13. Kidambi, S.; Dai, J.; Li, J.; Bruening, M. L. *Journal of the American Chemical Society* **2004**, 126, (9), 2658-2659.
- 14. Liu, J.; Cheng, L.; Song, Y.; Liu, B.; Dong, S. *Langmuir* **2001**, 17, (22), 6747-6750.
- 15. Watanabe, S.; Regen, S. L. Journal of the American Chemical Society 1994, 116, (19), 8855-6.
- 16. Scott, R. W. J.; Ye, H.; Henriquez, R. R.; Crooks, R. M. Chemistry of Materials **2003**, 15, (20), 3873-3878.
- 17. Krass, H.; Papastavrou, G.; Kurth, D. G. Chemistry of Materials **2003**, 15, (1), 196-203.
- 18. Kidambi, S.; Bruening, M. L. Chemistry of Materials 2005, 17, (2), 301-307.
- 19. Kumar, G.; Blackburn, J. R.; Albridge, R. G.; Moddeman, W. E.; Jones, M. M. *Inorganic Chemistry* **1972**, 11, (2), 296-300.
- 20. Semagina, N. V.; Bykov, A. V.; Sulman, E. M.; Matveeva, V. G.; Sidorov, S. N.; Dubrovina, L. V.; Valetsky, P. M.; Kiselyova, O. I.; Khokhlov, A. R.; Stein, B.; Bronstein, L. M. *Journal of Molecular Catalysis A: Chemical* **2004**, 208, (1-2), 273-284.
- 21. Yoon, C.; Yang, M. X.; Somorjai, G. A. Catalysis Letters 1997, 46, (1,2), 37-41.
- 22. Caruso, F.; Kurth, D. G.; Volkmer, D.; Koop, M. J.; Mueller, A. Langmuir 1998, 14, (13), 3462-3465.
- 23. Decher, G. Science 1997, 277, (5330), 1232-1237.

# Chapter 4. Multilayer Polyelectrolyte Films Containing Silver Nanoparticles As Anti-bacterial Membrane Coatings

### 4.1. Introduction

Membrane processes such as reverse osmosis, microfiltration, and nanofiltration are playing an increasing role in ensuring the availability of safe, potable water. However, one of the ubiquitous challenges in such technologies is minimization of membrane fouling by colloids, natural organic matter, and microbes. Formation of foulant layers results in a dramatic decline in membrane permeability over time, which leads to a higher energy demand (pressure) for a given volume of effluent. Biofouling is particularly difficult to control because even a few bacteria on a membrane surface can eventually multiply to form detrimental films. Moreover, waste generated by the organisms in a biofilm may damage membranes and possibly cause microbial contamination of permeate. 2.3

There are a number of strategies for overcoming biofouling, including pretreatment of the feed solution, 4, 5 modification of membrane surface properties (i.e., surface charge, hydrophobicity and roughness), 6-9 periodic cleaning, 10, 11 and surface functionalization with silver, 12-18 quaternary ammonium groups, 19-21, metals 22, 23 or chitosan 24-27. Silver has a long history as an antimicrobial agent and is particularly attractive for membrane modification because it possesses antibacterial properties for a wide spectrum of bacterial strains without being highly toxic to human cells. Additionally, microorganisms show a low tendency to develop resistance to silver-based products. 28 Silver ions readily bind to negatively charged components in proteins and

nucleic acids, thereby effecting structural changes in bacterial cell membranes and nucleic acids to decrease viability. In particular silver ions are thought to interact with thiol groups, phosphates, amino acids and key functional groups in enzymes, so that multiple deleterious interactions simultaneously interfere with microbial processes.<sup>29-32</sup>

In this chapter, we report work examining the antibacterial properties of Ag nanoparticle-containing multilayer polyelectrolyte films deposited on polyethersulfone ultrafiltration membranes. Several recent studies suggest that Ag nanoparticles have unique antibacterial properties,<sup>33, 34</sup> and deposition of polyelectrolyte multilayer provides a rapid, simple, and robust method for membrane modification.<sup>12</sup> Additionally, the use of multilayer polyelectrolyte films (MPFs) as a matrix for nanoparticles prevents particle aggregation and allows control over particle size. 12, 35-38 Rubner and others suggested that the mechanism of antibacterial action by Ag nanoparticles in polyelectrolyte films presumably involves oxidation of nanoparticles and slow release of Ag<sup>+,36,37,39</sup> In principle, this should lead to sustained life of membranes compared to films containing Ag<sup>+</sup> ions. Studies of silver leaching presented herein confirm that the rate of leaching of silver in Ag+-containing films is nearly an order of magnitude greater than that in Ag0nanoparticle containing systems, confirming that the use of Ag nanoparticles rather than ions could enhance the longevity of an antibacterial coating. Filtration of bacteriacontaining suspensions through modified membranes indicates that the flux decline associated with bacterial fouling in silver-containing films is lower than that in membranes without any silver coating, but it is difficult to distinguish between Ag+ and Ag<sup>0</sup>-containing films in short-term fouling studies.

#### 4.2. Experimental Section

#### 4.2.1. Materials.

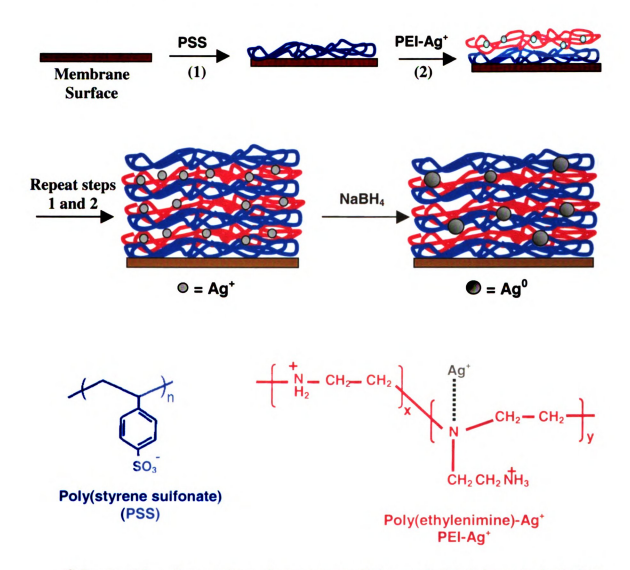
Polyethylenimine (PEI) (Aldrich,  $M_w = 25,000 \text{ Da}$ ), poly(styrene sulfonate) (PSS) (Aldrich, sodium salt,  $M_w = 70,000 \text{ Da}$ ), silver nitrate (99%, EM Science) and sodium borohydride (Aldrich) were used as received. The 50 kDa polyethersulfone (PES) membranes (Millipore, PBQK02510, 25 mm diameter) were immersed in water for 1 h to remove any impurities. Solutions were prepared with deionized water (Milli-Q, 18.2  $M\Omega$ cm).

### 4.2.2. Film Deposition on polyethersulfone membranes.

PSS/PEI deposition on water-cleaned PES supports began with immersion of the support in an aqueous solution containing 3 mg/mL PSS at pH 5 in 0.5 M NaCl for 10 min. PSS was always deposited first because hydrophobic interactions of PSS with PES are probably important for commencing adsorption. The PSS-coated polymer support was then rinsed with deionized water for 1 min before exposure to 1 mg/mL PEI at pH 6.5 for 5 min and another 1 min water rinse. This process was repeated until the desired number of bilayers was deposited, but after deposition of the initial bilayer, adsorption times for PSS were only 5 min.

Silver ions were incorporated into the polyelectrolyte films by employing a PEI-Ag<sup>+</sup> complex (1 mg/mL PEI, 10 mM AgNO<sub>3</sub>, with no pH adjustment) instead of PEI in the film deposition procedure. The pH of this solution was about 6.1. After deposition of the entire film, Ag<sup>+</sup> ions were reduced in 0.1 M NaBH<sub>4</sub> for 10 min, followed by rinsing

with distilled water for 1 min, to yield antibacterial Ag nanoparticles embedded in a polyelectrolyte multilayer film (scheme 4.1).



#### 4.2.3. Film Characterization.

Films (4.5 bilayers) were also deposited on carbon-coated copper grids for TEM imaging. Prior to film deposition, which occurred as described above, the grids were cleaned in a UV/ozone cleaner for 1 min, and TEM was performed on a JEOL-2010F Field-Emission microscope operating at 100kV. The digital images were taken with a Mega View III Soft Imaging System. External reflectance FTIR spectra of films were obtained with a Nicolet Magna-IR 560 spectrometer using a Pike grazing angle (80°) attachment.

#### 4.2.4. Leaching of Ag from multilayer films on polymer supports.

To determine the amount of Ag<sup>+</sup> leached from different membranes, 50kDa PES filters coated with (PSS/PEI-Ag<sup>+</sup>)<sub>4</sub>/PSS or (PSS/PEI-Ag<sup>0</sup>)<sub>4</sub>/PSS were immersed in sterile Luria-Bertani (LB) nutrient broth (2.5 mL), which was replaced at regular intervals. We used a higher concentration of silver during deposition (100 mM) for the leaching experiments to ensure the detection of the leached silver. The broth samples were analyzed by Atomic absorption spectroscopy (AAS) to determine the amount of Ag they contained, and after leaching studies, 2 mL of concentrated HNO<sub>3</sub> was added to the membranes to extract the remaining silver. This extract was diluted with 8 mL of 0.1 M HNO<sub>3</sub> and analyzed using AAS. Standards for the analysis were prepared in LB broth for leached samples, and in 0.1 M HNO<sub>3</sub> for extracted samples.

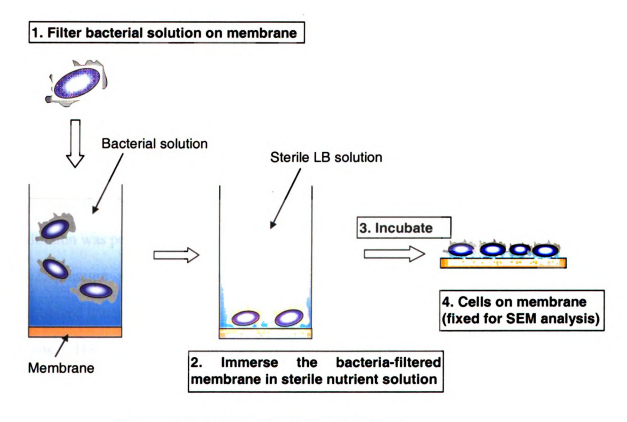
#### 4.2.5. Bacteria and culture conditions.

E. coli JM109 cells (Stratagene, Catalog #200235) were cultivated in LB broth (10 g of tryptone, 5 g of yeast extract, 5 g NaCl per L) in an incubator shaker (250 rpm) at 37 °C. The bacterial suspension, which was cultured overnight, was then diluted (1 mL in100 mL) with fresh LB broth, and further cultivated to mid-logarithmic phase when optical density reaches 0.6-0.8. The number of bacterial cells was then adjusted to approximately  $5\times10^8$  cells per mL (optical density at 600 nm of  $\sim0.5$ )<sup>40</sup> in LB broth. Cells were collected by centrifugation (10 min, 3000 rpm), and then resuspended in sterile water ( $5\times10^8$  cells per mL of water).

## 4.2.6. Examination of the Inhibition of Bacterial Growth by Scanning Electron Microscopy (Scheme 4.2).

PES membranes coated with (PSS/PEI)<sub>4</sub>/PSS, (PSS/PEI-Ag<sup>+</sup>)<sub>4</sub>/PSS, and (PSS/PEI-Ag<sup>0</sup>)<sub>4</sub>/PSS films were used to filter 3 mL of bacterial suspension (*E. Coli* JM109) in sterile water (bacteria grown for 18 h at 37 °C in LB were collected by centrifugation and then resuspended in water, which is then diluted to ~10<sup>7</sup> cells/mL with sterile deionized water). Because the bacteria (micron dimensions) are much bigger than the pore diameters in 50 kDa PES membranes, all the bacteria should be retained on the membrane surface to ensure that the same amounts of bacteria are deposited on all samples. After filtration (the membranes were not rinsed), these bacteria-coated membranes were incubated in 2.5 mL of LB broth for 3 days, dabbed lightly on a Kim wipe, and rinsed briefly for 3 s using deionized water to remove any broth and unadhered bacteria from the membrane. To preserve the bacterial structures, the adhered bacteria

were fixed on the membrane using a 30 min exposure to a formaldehyde/glutaraldehyde mixture (2.5 volume % each in 0.1 M sodium cacodylate buffer, pH 7.4; Catalog #15949) obtained from Electron Microscopy Sciences. The fixed samples were then rinsed in distilled water and dehydrated by sequential 15-min immersions in solutions containing increasing concentrations of ethanol (25, 50, 75, and 95 % (v/v)). The final dehydration step involved three 5-min immersions with 100% ethanol (to fasten the drying process), after which the samples were air-dried, sputter coated with a thin (5 nm) layer of gold, and observed using a field emission scanning electron microscope (JEOL 6300F, Japan).



Scheme 4.2: Initial assay of bacterial growth.

#### 4.2.7. Examination of the Inhibition of Bacterial Growth by Optical Microscopy.

In collabroation with Dr. Viktoriya Konovalova of Kyiv Mohyla Academy, we also verified antibacterial properties using optical microscopy, which provides a wider field of view. Antimicrobial activity was determined against gram-negative *Escherichia coli* HB 101 that were purchased from the Ukrainian Collections of Microorganisms. The bacteria were grown on agar containing Nutrient Broth No.1 (Fluka), and microbial suspensions were collected in sterilized 0.9% NaCl. The concentration of *E. coli* was about 80 cells/mL. 50 mL of suspension was then filtered through 50 kDa PES membrane (44.5 mm diameter, Microdyn-Nadir, Wiesbaden, Germany) at a transmembrane pressure of 2 bar. The membranes were then incubated on Endo agar plates (Fluka) for 24 h-28 days at 30°C.

#### 4.2.8. Long-term Dead-end Filtration of Bacterial Suspensions.

We performed filtration of bacterial suspensions using the coated membranes to examine the ability of the polyelectrolyte films to resist bacterial fouling. Dead-end filtration was performed with a stirred filtration cell (Amicon model 8010) connected to a 5 L pressure vessel. In this case, we compacted the bare membranes by filtering deionized water under a pressure of 4.8 bar for about 15 h before building the multilayer films. The compacted membranes were then coated with multilayer films using the method described earlier. We determined the pure water and bacterial fluxes through the coated membranes as a function of time using an analytical balance. Analyses were made at constant pressure (4.8 bar) and also at approximately constant initial flux values

for the different membrane systems. LabView software was employed for the continuous collection of flux data

#### 4.3. Results and Discussion

#### 4.3.1. Layer-by-layer growth of polyelectrolyte using reflectance FT-IR.

The growth of PSS/PEI films on Au occurs in a controlled layer-by layer fashion. We begin the film formation by immersing an Au-coated wafer into a solution of PEI to allow the adsorption of PEI. Subsequent alternating immersions in PSS and PEI solutions produce a multilayer film. External reflection FTIR spectra (Figure 4.1) demonstrate the layer-by-layer growth of these coatings as absorbance values of peaks at 1033 cm<sup>-1</sup> (corresponding to sulfonate peak of PSS) and 1010 cm<sup>-1</sup> (attributed to a ring vibration of PSS), increase regularly with the number of deposited bilavers. 42

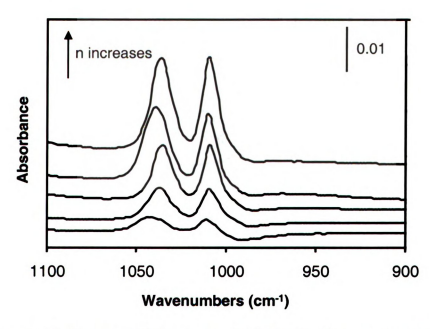


Figure 4.1. Reflectance FTIR spectra of [PEI/PSS]<sub>n</sub> films on Au with n varying from 1-5.

#### 4.3.2. Film Characterization.

To examine nanoparticle formation by reduction of Ag<sup>+</sup>, we obtained TEM images of films deposited on a carbon-coated Cu grid. The TEM image in Figure 4.2 confirms the formation of Ag nanoparticles during exposure of (PSS/PEI-Ag<sup>+</sup>)<sub>d</sub>/PSS films to NaBH<sub>4</sub> and shows that the particles have diameters of ~60 nm. Previous TEM analysis of reduced (poly(acrylic acid)/PEI-Ag<sup>+</sup>)<sub>d</sub>/poly(acrylic acid) films showed formation of particles with diameters of only 4 nm when using 0.5 mM Ag<sup>+</sup> during the PEI deposition.<sup>12</sup>

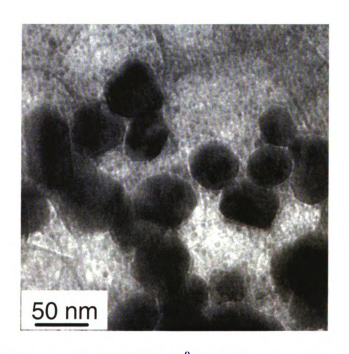


Figure 4.2. TEM image of a (PSS/PEI-Ag  $^0)_4/PSS$  film on a carbon-coated copper grid.

The particles in Figure 4.2 are 15-fold larger in diameter than those previously formed in poly(acrylic acid)/PEI films because a higher concentration of Ag<sup>+</sup> ions was used during film deposition (10 mM), and perhaps more importantly because the PSS/PEI films are likely more permeable to ions due to a lower density of ionic cross-links.<sup>43</sup> This higher permeability allows more Ag<sup>+</sup> ions to aggregate during reductive formation of nanoparticles.

#### 4.3.3. Evaluation of Anti-microbial properties using Microscopy.

Figure 4.3 presents SEM images of PES membranes that were treated by filtration of 3 mL of *E. Coli* solution (~10<sup>7</sup> cells/mL), incubation in LB broth for 18 h, and fixation of the bacteria (Scheme 4.2). Figure 4.3 clearly shows bacterial growth on the entire surface of the membrane coated with (PSS/PEI)<sub>4</sub>/PSS. In contrast, essentially complete inhibition of growth is observed on the membranes coated with films containing Ag<sup>+</sup> and Ag<sup>0</sup>. Both types of Ag-containing samples possess antibacterial properties and likely kill *E. Coli* cells at an early stage of biofilm formation.

We also verified antibacterial properties using optical microscopy, which provides a wider field of view. In this case, the bacteria were cultured in Endo medium (Fluka), which contains fuchsin-sulfite that reacts with the acid and aldehyde groups in bacteria to yield a pink color. In the membranes without silver, there are sufficient acid and aldehyde moieties from the bacterial colonies to stain the entire membrane, and colonies appears as brighter pink spots. In contrast, membranes coated with Ag<sup>0</sup>- and Ag<sup>+</sup>- containing films have 100% antibacterial properties even after 10 days of incubation, as shown in Figure 4.4 where no bacterial colonies are visible on the Ag-containing

membranes. (The white outer ring on the membranes results from an o-ring that prevented both films deposition and bacterial filtration in this area.) Micrographs similar to those in Figure 4.4 were also obtained after 28 days of incubation.

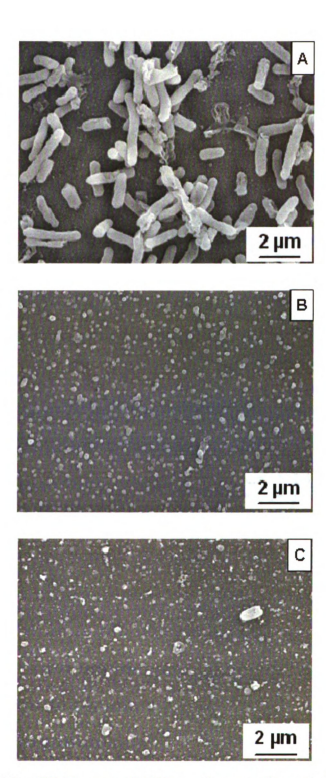
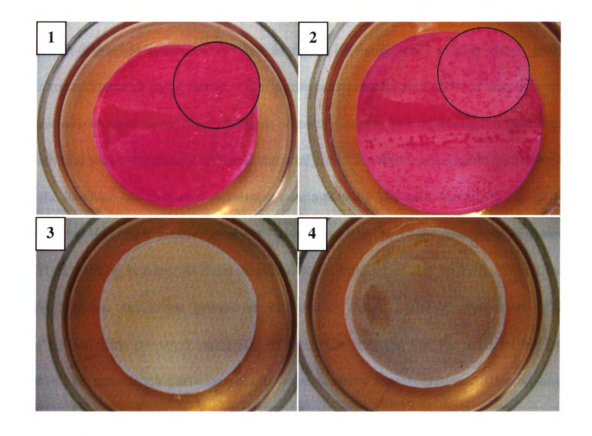


Figure 4.3: SEM images of PES membrane surfaces that were coated with (PSS/PEI)<sub>4</sub>/PSS (A), (PSS/PEI-Ag<sup>+</sup>)<sub>4</sub>/PSS (B), or (PSS/PEI-Ag<sup>0</sup>)<sub>2</sub>/PSS (C) and subsequently treated by filtration of 3 mL of bacteria (10<sup>7</sup> cells/mL), incubation in LB broth for 18 h, and fixation of bacteria with a formaldehyde/glutaraldehyde mixture.



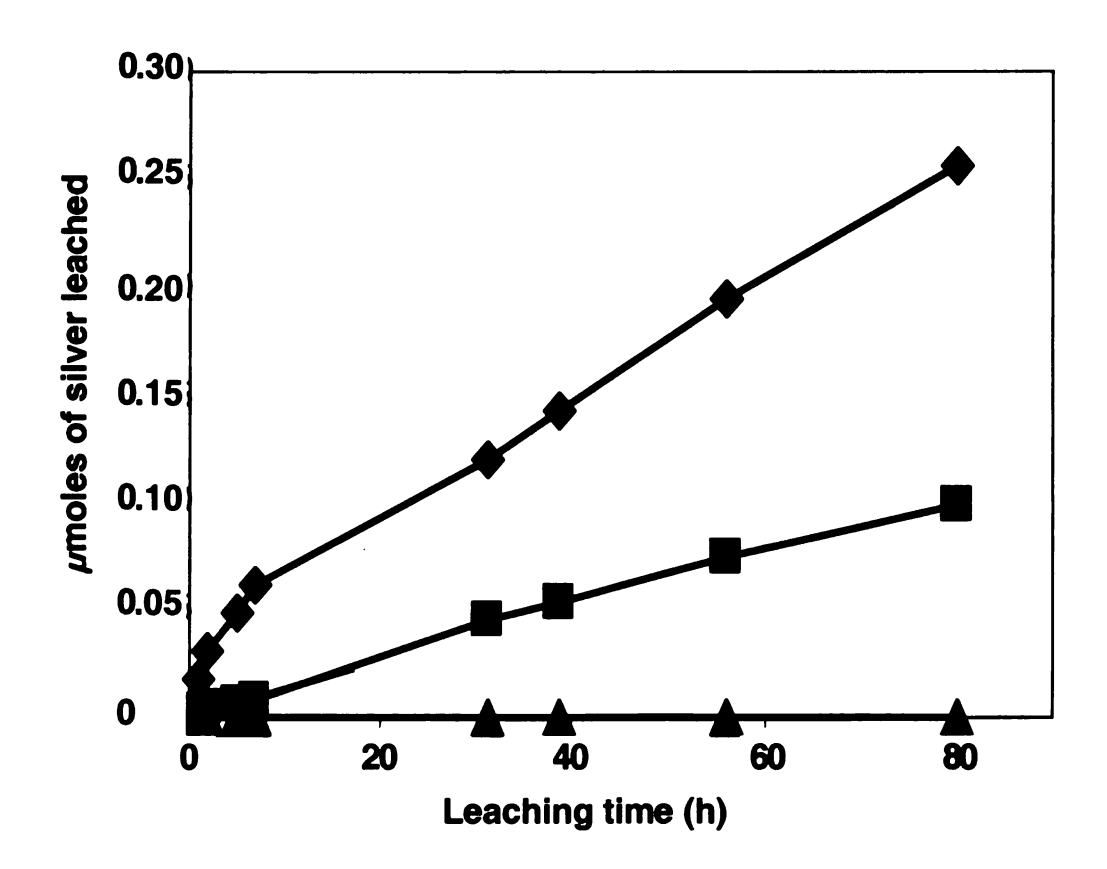
**Figure 4.4.** Optical micrographs of PES membranes that were uncoated (1-control), or coated with (PSS/PEI)<sub>2</sub>/PSS (2), (PSS/PEI-Ag<sup>6</sup>)<sub>2</sub>/PSS (3), or (PSS/PEI-Ag<sup>6</sup>)<sub>2</sub>/PSS (4), and subsequently used to filter 3 mL of bacterial suspensions prior to incubation in Endo medium for 10 days. (Figure courtesy of Dr. Viktoriya Konovalova)

#### 4.3.4. Leaching of Ag from multilayer films on polymer supports.

The antibacterial properties of polyelectrolyte films containing silver (Ag<sup>+</sup> or Ag<sup>0</sup>) should depend on both the amount of silver immobilized in the coating and the rate of leaching of Ag<sup>+</sup> into the surrounding medium. Hence, evaluation of the amount of Ag deposited and the rate of leaching will be vital in understanding the efficacy and duration of antibacterial properties. Because Ag<sup>+</sup> leaching rates from nanoparticle-containing films in deionized water are very low as shown by the Kotov<sup>44</sup> and Bayston<sup>33</sup> groups, we examined leaching in LB broth. (Our preliminary results also showed very low leaching rates in deionized water.) Experiments were carried out by immersing the membrane into broth that was periodically changed and analyzed. To obtain analyzable quantities of Ag<sup>+</sup> in the leachate, we prepared membrane coatings using 100 mM AgNO<sub>3</sub> in PEI deposition solutions. (There is an excess of Ag<sup>+</sup> with respect to the amine groups of PEI when 100 mM of AgNO<sub>3</sub> is used, so there could be some binding of Ag<sup>+</sup> to PSS. When using 10 mM AgNO<sub>3</sub>, the amine groups of PEI are in excess.) TEM images of (PSS/PEI-Ag<sup>0</sup>)<sub>4</sub>/PSS films prepared using 100 mM AgNO<sub>3</sub> indicate that the sizes of the particles are ~ 250 nm. Such particles should be reasonably representative of the 60 nm silver nanoparticles that were used for the other experiments.

Figure 4.5 shows the results from AAS analysis of LB solutions containing silver that was leached from 50 kDa PES membranes coated with (PSS/PEI-Ag<sup>+</sup>)<sub>4</sub>/PSS or (PSS/PEI-Ag<sup>0</sup>)<sub>4</sub>/PSS films. The data indicate that the initial rate of leaching of silver (<10 h of leaching time) from (PSS/PEI-Ag<sup>+</sup>)<sub>4</sub>/PSS-coated membranes is about 7-fold higher than that from (PSS/PEI-Ag<sup>0</sup>)<sub>4</sub>/PSS-coated membranes. Afterward the rate of leaching from the Ag<sup>+</sup> containing membrane was only 3-fold greater than that from the

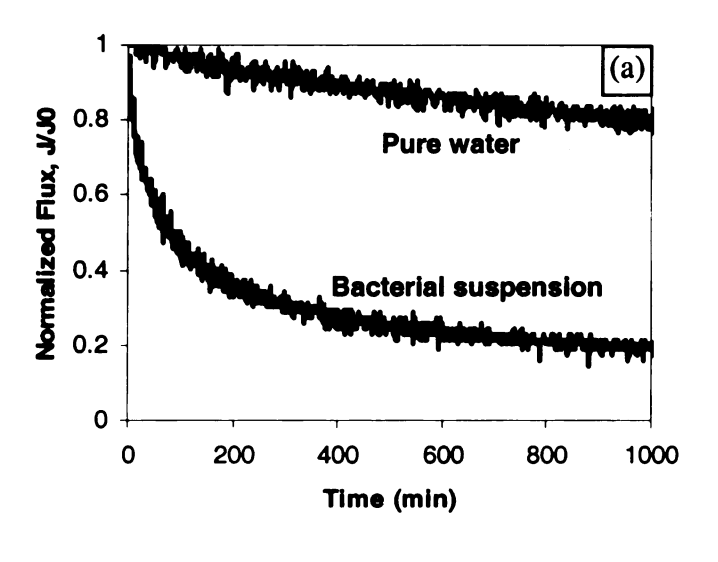
nanoparticle membranes. (Of course, the control experiment with a PES membrane coated with (PSS/PEI)<sub>4</sub>/PSS indicated the absence of silver in that system.) We also analyzed the amounts of silver remaining on the membranes after the leaching experiments by extracting the silver using nitric acid. In the case of the Ag<sup>+</sup> system, we observed that about 40% of the total silver remained in the membrane after leaching with LB broth for ~70-80 h, while ~80% of the total silver remained in Ag<sup>0</sup> system. The total amount of Ag in the two types of membranes was about the same (0.4 micromoles). Also, by extracting the silver from a new batch of coated membranes (without any leaching), we verified that the sum of the amount of silver leached and the amount of silver loaded. From these studies, we conclude that reduction of the silver to form nanoparticles can potentially provide a more sustained release of silver to give longer-lasting antibacterial activity.

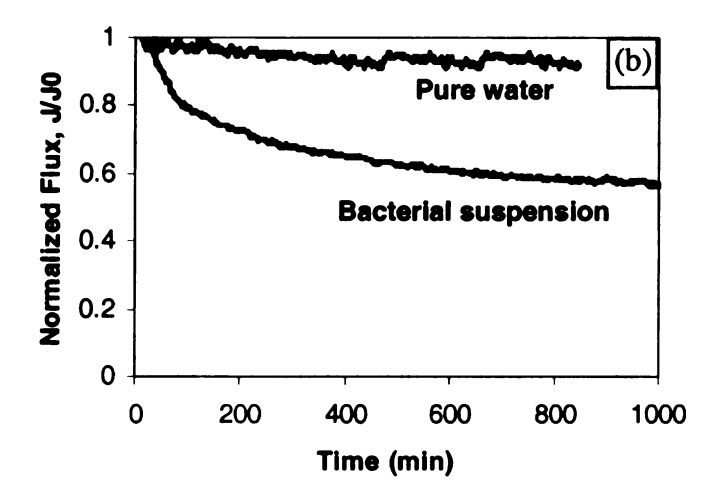


**Figure 4.5**. Amount of silver leached from PES membranes coated with  $(PSS/PEI)_4/PSS$  ( $\triangle$ ),  $(PSS/PEI-Ag^+)_4/PSS$  ( $\diamondsuit$ ), and  $(PSS/PEI-Ag^0)_4/PSS$  ( $\blacksquare$ ) during immersion in LB broth without stirring. Broth samples were analyzed by AAS.

#### 4.3.5. Changes in Flux during Filtration of Bacterial Suspensions.

To demonstrate whether Ag-containing coatings can retard biofouling, we also examined flux declines during filtration of solutions containing bacteria. Unfortunately, to achieve large flux declines within a few h, we had to employ bacterial suspensions containing high concentrations of bacteria (about 10<sup>8</sup> cells/mL). To ensure that flux declines were primarily due to fouling and not membrane compaction, bare membranes were compacted at 4.8 bar with pure water for 15 h prior to coating with polyelectrolyte films. When we measured pure water flux through such coated membranes over a period of 15 h, we saw only small (<15%) flux declines that may result from compaction of the polyelectrolyte coatings or light fouling due to adventitious contaminants in the system. Upon filtration of bacterial suspensions, however, flux through a (PSS/PEI)4/PSS-coated membrane declined by 80% over 15 h, whereas, in the case of (PSS/PEI-Ag<sup>+</sup>)<sub>4</sub>/PSS- and (PSS/PEI-Ag<sup>0</sup>)<sub>4</sub>/PSS-coated membranes, there was only a 40-50% decline in flux over the same time period as shown in Figure 4.6. We repeated the filtration experiments using three different membranes, and the percentage decline in the flux is reproducible within 10% from each run. Consistent with this result, FESEM images of the membrane surfaces after bacterial filtration (Figure 4.7) show a much higher concentration of bacterial deposits on the (PSS/PEI)<sub>4</sub>/PSS-coatings, than on silver-containing membranes.





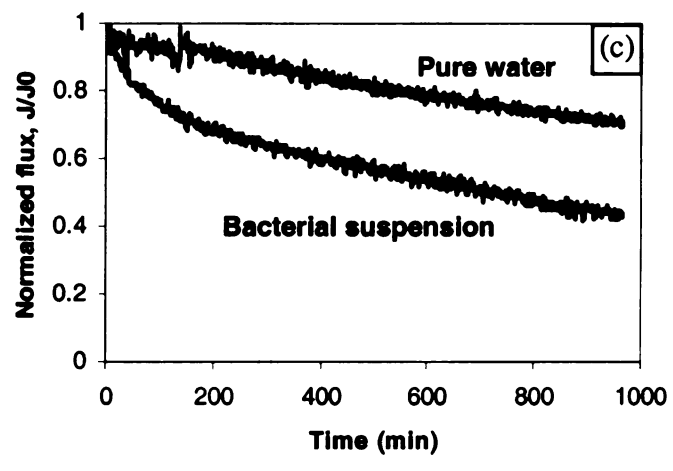


Figure 4.6. Temporal flux profiles during filtration of deionized water or bacterial suspensions (10<sup>8</sup> cells/mL of deionized water) through PES membranes coated with (PSS/PEI)<sub>4</sub>/PSS (a), (PSS/PEI-Ag<sup>+</sup>)<sub>4</sub>/PSS (b), and (PSS/PEI-Ag<sup>0</sup>)<sub>4</sub>/PSS (c). The transmembrane pressure was 4.8 bar.

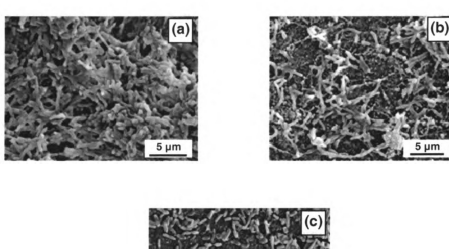




Figure 4.7 : SEM images of PES membranes that were coated with (PSS/PEI) $_d$ PSS (a), (PSS/PEI-Ag $^1$ ) $_d$ PSS (b), or (PSS/PEI-Ag $^1$ ) $_d$ PSS (c) and subsequently used to filter a bacterial suspension (10 $^8$  cells/mL) for 15-16 h. Bacteria were fixed with glutaraldehyde prior to imaging.

Unfortunately, interpretation of these constant pressure (4.8 bar) experiments is complicated by the fact that the initial flux is not the same among the different membranes (Figure 4.8). The higher initial flux through the (PSS/PEI)<sub>4</sub>/PSS-coated membrane could contribute to its more rapid fouling. Thus, we also reduced the pressure on the (PSS/PEI)<sub>4</sub>/PSS-coated membrane from 4.8 to 2.4 bar to better compare these membranes with those containing Ag. Figure 4.9 indicates that even at the reduced pressure the flux decline through the (PSS/PEI)<sub>4</sub>/PSS-containing membranes was still 78% or nearly double that through the Ag-containing membranes.

Comparison of the Ag<sup>+</sup> and Ag<sup>0</sup> nanoparticle-containing membranes is difficult. Both reduce fouling, but at these high concentrations of bacteria, silver is not released rapidly enough to kill all of the cells. Moreover, a higher rate of release of Ag<sup>+</sup> may be advantageous in short-term studies but deleterious in the long-term. Long-term fouling studies (weeks at least) with lower bacteria concentrations will be needed to address whether nanoparticle-containing films are more effective in providing long-term resistance to fouling.

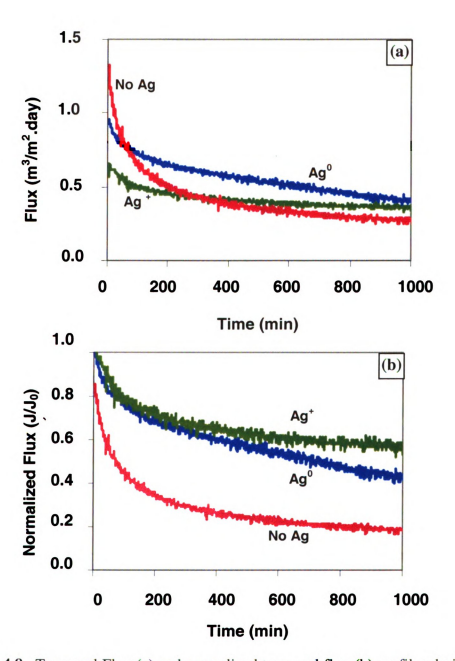
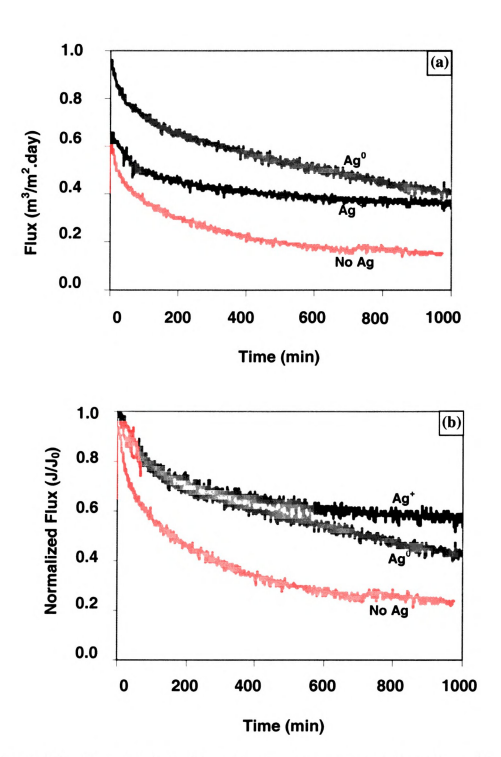


Figure 4.8. Temporal Flux (a) and normalized temporal flux (b) profiles during bacteria filtration with PES membranes modified with different coatings at a constant pressure of 4.8 bar. (PSS/PEI)-Ag\*)\_#/PSS-green, and (PSS/PEI-Ag\*)\_#/PSS-blue. The feed filtration solutions initially contained 108 cells/mL.



**Figure 4.9.** Temporal Flux (a) and normalized temporal flux (b) profiles during filtration of bacterial solutions through PES membranes coated with (PSS/PEI)<sub>4</sub>/PSS-red; (PSS/PEI-Ag\*)<sub>4</sub>/PSS-green, and (PSS/PEI-Ag\*)<sub>4</sub>/PSS-blue. The feed filtration solutions initially contained 10<sup>8</sup> cells/mL, and filtration pressures were selected to give similar initial flux values (see text).

## 4.4. Conclusions.

The layer-by-layer deposition of PSS and PEI-Ag $^+$  on PES membranes and subsequent reduction of Ag $^+$  using NaBH $_4$  is a versatile method for synthesizing antibacterial silver nanoparticles on the surface of filtration membranes. SEM images and filtration of bacterial suspensions indicate that silver (both Ag $^+$  and Ag $^0$  systems) immobilized in membranes can serve as an effective antibacterial agent. The initial rate of leaching of silver in Ag $^+$  systems is about 7-fold faster than that in Ag $^0$ -containing films, which indicates that Ag $^0$  can potentially have a sustained life as an antibacterial system relative to Ag $^+$ -containing membranes.

#### 4.5. References

- 1. Reissmann, F. G.; Uhl, W. Desalination 2006, 198, (1-3), 225-235.
- 2. Rose, A. H.; Editor, *Economic Microbiology, Vol. 6: Microbial Biodeterioration*. 1981; p 516 pp.
- 3. Geesey, G. G.; Lewandowski, Z.; Flemming, H.-C.; Editors, *Biofouling and Biocorrosion in Industrial Water Systems*. 1994; p 297 pp.
- 4. Dudley, L. Y.; Darton, E. G. Desalination 1997, 110, (1-2), 11-20.
- 5. Ma, W.; Zhao, Y.; Wang, L. Desalination 2007, 203, (1-3), 256-259.
- 6. Allion, A.; Baron, J.-P.; Boulange-Petermann, L. *Biofouling* **2006**, 22, (5), 269-278.
- 7. Gan, D.; Mueller, A.; Wooley, K. L. Journal of Polymer Science, Part A: Polymer Chemistry 2003, 41, (22), 3531-3540.
- 8. Norberg, D.; Hong, S.; Taylor, J.; Zhao, Y. Desalination **2007**, 202, (1-3), 45-52.
- 9. Pasmore, M.; Todd, P.; Smith, S.; Baker, D.; Silverstein, J.; Coons, D.; Bowman, C. N. Journal of Membrane Science 2001, 194, (1), 15-32.
- 10. Kwak, S.-Y.; Kim, S. H.; Kim, S. S. Environmental Science and Technology **2001**, 35, (11), 2388-2394.
- 11. Zhao, Y.-J.; Wu, K.-F.; Wang, Z.-J.; Zhao, L.; Li, S.-S. *Journal of Environmental Sciences (China)* **2000**, 12, (2), 241-251.
- 12. Dai, J.; Bruening, M. L. *Nano Letters* **2002**, 2, (5), 497-501.
- 13. Gray, J. E.; Norton, P. R.; Alnouno, R.; Marolda, C. L.; Valvano, M. A.; Griffiths, K. *Biomaterials* **2003**, 24, (16), 2759-2765.
- 14. Grunlan, J. C.; Choi, J. K.; Lin, A. Biomacromolecules 2005, 6, (2), 1149-1153.

- 15. Ignatova, M.; Labaye, D.; Lenoir, S.; Strivay, D.; Jerome, R.; Jerome, C. Langmuir 2003, 19, (21), 8971-8979.
- 16. Jansen, B.; Kohnen, W. Journal of Industrial Microbiology 1995, 15, (4), 391-6.
- 17. Lee, H. J.; Yeo, S. Y.; Jeong, S. H. *Journal of Materials Science* **2003**, 38, (10), 2199-2204.
- 18. Shi, Z.; Neoh, K. G.; Kang, E. T. *Langmuir* **2004**, 20, (16), 6847-6852.
- 19. Cen, L.; Neoh, K. G.; Kang, E. T. *Langmuir* **2003**, 19, (24), 10295-10303.
- 20. Nakagawa, Y.; Hayashi, H.; Tawaratani, T.; Kourai, H.; Horie, T.; Shibasaki, I. Applied and Environmental Microbiology 1984, 47, (3), 513-18.
- 21. Tiller, J. C.; Liao, C.-J.; Lewis, K.; Klibanov, A. M. Proceedings of the National Academy of Sciences of the United States of America 2001, 98, (11), 5981-5985.
- 22. Fu, G.; Vary, P. S.; Lin, C.-T. Journal of Physical Chemistry B 2005, 109, (18), 8889-8898.
- 23. Stoimenov, P. K.; Klinger, R. L.; Marchin, G. L.; Klabunde, K. J. *Langmuir* **2002**, 18, (17), 6679-6686.
- 24. Fu, J.; Ji, J.; Yuan, W.; Shen, J. Biomaterials **2005**, 26, (33), 6684-6692.
- 25. Huh, M. W.; Kang, I.-K.; Lee, D. H.; Kim, W. S.; Lee, D. H.; Park, L. S.; Min, K. E.; Seo, K. H. *Journal of Applied Polymer Science* **2001**, 81, (11), 2769-2778.
- 26. Lim, S.-H.; Hudson, S. M. *Journal of Macromolecular Science, Polymer Reviews* **2003**, C43, (2), 223-269.
- 27. Rabea, E. I.; Badawy, M. E. T.; Stevens, C. V.; Smagghe, G.; Steurbaut, W. Biomacromolecules 2003, 4, (6), 1457-1465.
- 28. Percival, S. L.; Bowler, P. G.; Russell, D. The Journal of hospital infection 2005, 60, (1), 1-7.

- 29. Butkus, M. A.; Edling, L.; Labare, M. P. Journal of Water Supply: Research and Technology-AQUA 2003, 52, (6), 407-416.
- 30. Holt, K. B.; Bard, A. J. Biochemistry **2005**, 44, (39), 13214-13223.
- 31. Liau, S. Y.; Read, D. C.; Pugh, W. J.; Furr, J. R.; Russell, A. D. Letters in Applied Microbiology 1997, 25, (4), 279-283.
- 32. McDonnell, G.; Russell, A. D. Clinical Microbiology Reviews 1999, 12, (1), 147-179.
- 33. Furno, F.; Morley, K. S.; Wong, B.; Sharp, B. L.; Arnold, P. L.; Howdle, S. M.; Bayston, R.; Brown, P. D.; Winship, P. D.; Reid, H. J. *Journal of Antimicrobial Chemotherapy* **2004**, 54, (6), 1019-1024.
- 34. Sondi, I.; Salopek-Sondi, B. *Journal of Colloid and Interface Science* **2004**, 275, (1), 177-182.
- 35. Kidambi, S.; Dai, J.; Li, J.; Bruening, M. L. *Journal of the American Chemical Society* **2004**, 126, (9), 2658-2659.
- 36. Lee, D.; Cohen, R. E.; Rubner, M. F. Langmuir 2005, 21, (21), 9651-9659.
- 37. Li, Z.; Lee, D.; Sheng, X.; Cohen, R. E.; Rubner, M. F. *Langmuir* **2006**, 22, (24), 9820-9823.
- 38. Kidambi, S.; Bruening, M. L. Chemistry of Materials 2005, 17, (2), 301-307.
- 39. Tredget, E. E.; Shankowsky, H. A.; Groeneveld, A.; Burrell, R. The Journal of burn care & rehabilitation 1998, 19, (6), 531-7.
- 40. Lehtinen, J.; Nuutila, J.; Lilius, E.-M. Cytometry, Part A 2004, 60A, (2), 165-172.
- 41. Xu, W.; Chellam, S. Environmental Science and Technology 2005, 39, (17), 6470-6476.
- 42. Malaisamy, R.; Bruening, M. L. Langmuir 2005, 21, (23), 10587-10592.

- 43. Harris, J. J.; Stair, J. L.; Bruening, M. L. Chemistry of Materials 2000, 12, (7), 1941-1946.
- 44. Podsiadlo, P.; Paternel, S.; Rouillard, J.-M.; Zhang, Z.; Lee, J.; Lee, J.-W.; Gulari, E.; Kotov, N. A. *Langmuir* **2005**, 21, (25), 11915-11921.

## **Chapter 5: Conclusions and Future Work**

This thesis demonstrates that metal nanoparticles can be easily incorporated in PEMs by the deposition of metal ions in polyelectrolyte films followed by reduction. These nanoparticle-containing films are versatile, thin nanocomposites for developing applications in selective catalysis and antibacterial coatings. The multilayers help in stabilizing the nanoparticles and can still maintain important properties of the Pd (catalytic) and silver (antibacterial) nanoparticles. Also, the technique of layer by layer deposition allows good control over the properties of the multilayers through tuning of the deposition conditions such as pH, ionic strength and number of bilayers, and through selection of the polyelectrolyte(s) for the multilayer growth. Specifically, we observed that the catalytic properties of Pd nanoparticles change based on the nature of the multilayer system in which they are encapsulated, and on the number of bilayers that are deposited.

# 5.1. Incorporation of metal nanoparticles in polyelectrolyte multilayer films for selective catalysis

In Chapter 2, we have seen that synthesis of [PAA/PEI-Pd(0)]<sub>n</sub>PAA films occurs through alternating immersions of alumina particles in solutions of PAA and a PEI-Pd(II) complex, followed by reduction of Pd(II) by NaBH<sub>4</sub> to give Pd nanocatalysts in a PAA/PEI film. Pd nanoparticles encapsulated in polymer films thus formed are not only active, but also selective during hydrogenation of structurally similar molecules. In Chapter 3, a new catalytic system that is prepared by alternating immersions of a substrate in PdCl<sub>4</sub><sup>2-</sup> and PEI solutions followed by reduction of Pd(II) was examined. In

both these systems, the rates of hydrogenation of smaller molecules were higher than those of bigger molecules, presumably because of their faster transport to catalytic sites.

## 5.2. Application of Ag nanoparticles in polyelectrolyte multilayer films as antibacterial coatings

Bacterial fouling is a severe problem in membrane processes because it results in a dramatic decline in membrane permeability, which leads to a higher energy demand (pressure) for a given volume of effluent. Thus, it is best to prevent biofilm formation at its earliest stages. In Chapter 4, we have examined the use of Ag nanoparticle-containing multilayer polyelectrolyte films deposited on ultrafiltration membranes as agents that prevent bacteria deposition and growth. Alternating adsorption of PSS and a PEI-Ag<sup>+</sup> complex on the ultrafiltration substrates and subsequent reduction of Ag<sup>+</sup> by NaBH<sub>4</sub> yield antibacterial Ag nanoparticles embedded in multilayer polyelectrolyte films. The mechanism of antibacterial action by the nanoparticles presumably involves oxidation and slow release of Ag<sup>+</sup> ions, which should result in longer-lasting anti-fouling properties for reduced [PEI-Ag<sup>+</sup>/PSS]<sub>4</sub> relative to unreduced [PEI-Ag<sup>+</sup>/PSS]<sub>4</sub> coatings.

## 5.3. Future Work: Selective Catalysis

The work reported in Chapters 2 and 3 focused on studying selective hydrogenation among different molecules. It will be interesting and beneficial to analyze selective hydrogenation within a molecule. This is vital in syntheses where attainment of the desired product requires hydrogenation of one functional group in the presence of

others. For instance, the selective partial hydrogenation of a carbon-carbon triple bond of dehydrolinalool to a double bond is preferred in the synthesis of linalool, which has many commercial applications, particularly in perfume industry.<sup>1</sup>

#### 5.3.1. Selective hydrogenation of dienes

There is always a necessity for selective hydrogenation of alkenes with multiple carbon-carbon double bonds, and this has encouraged the development of a variety of catalysts like Wilkinson's catalyst (tris(triphenyl-phosphine)rhodium(I) chloride)<sup>2</sup> that prefer to hydrogenate a less hindered olefinic bond. In the presence of Wilkinson's catalyst, the rate of hydrogenation of 1-hexene in benzene is 1.1 and 49 times higher than that for 2-methylpent-1-ene and 1-methylcyclohexene,<sup>3</sup> respectively. Our group has done some preliminary work indicating that the immobilized nanoparticle catalysts are ideal candidates for selective hydrogenation of monosubstituted double bonds, and this could branch out to the detailed study of various other compounds of industrial/pharmaceutical significance.

#### 5.3.2. Synergistic effect using bimetallics

Bimetallic nanoparticles have electronic properties that are not available with a single metal and thus, these materials are attractive for developing new materials with unique catalytic properties. To date, the preparation of bimetallic nanoparticles has been carried out mainly on mineral supports, and the resulting inorganic oxide-supported bimetallic nanoparticles have already been used as effective catalysts for various

reactions.<sup>4</sup> However, synthesis of bimetallics can be easily achieved by reduction of metal ions in polyelectrolyte films, and the composition of catalyst should be readily controlled.

Prior research on hydrogenation of nitroaromatics to the corresponding aromatic amines, showed that a monometallic PVPy (poly(*N*-vinyl-2-pyrrolidone))-Pd catalyst exhibits mild or poor activity, but similar bimetallic palladium-platinum catalysts, PVPy-Pd-1/4Pt, exhibit very high activity and selectivity.<sup>5</sup> Similarly, higher catalytic activity and selectivity were observed with bimetallic nanoparticles containing Pd (PdAu, PdPt) during the selective (partial) hydrogenation of dehydrolinalool to linalool.<sup>1</sup> Incorporation of a second metal often modifies the properties of the nanoparticles, increasing the activity of the catalysts. This can be caused by a change in the electronic structure of the main metal (Pd), by a change in the morphology of the particle, or by some other changes.<sup>6</sup> Thus, it would be interesting to study the synergistic effect of bimetallic nanoparticles embedded in polyelectrolytes, since we can prepare these bimetallics by simply complexing the polycations with two types of polycations during deposition. Thus, we can have control over the composition of the bimetallic nanoparticles.

## 5.4. Future Work: Antibacterial Coatings

A recent report by Pal *et al.* showed that the antibacterial properties of Ag nanoparticles may vary with their size and shape.<sup>7</sup> It would be worth investigating the effect of shape and size of silver nanoparticles encapsulated in PEMs on the antibacterial activity of the system.

Apart from silver, there are also several other potential nanomaterials, e.g., titanium oxide, 8-10 zinc oxide 11, 12 and copper, 13 that have recently been shown to impart antibacterial properties. PEMs can be easily employed in incorporating these nanomaterials for desired antibacterial applications.

### 5.5. Summary Statement.

This thesis has shown that nanoparticles encapsulated in polyelectrolyte films can be employed in various applications, particularly in catalysis and as antifouling agents. There is tremendous potential for this science to expand and grow into other research areas depending upon the applications in consideration.

#### 5.6. References.

- 1. Bronstein, L. M.; Chernyshov, D. M.; Volkov, I. O.; Ezernitskaya, M. G.; Valetsky, P. M.; Matveeva, V. G.; Sulman, E. M. *Journal of Catalysis* **2000**, 196, (2), 302-314.
- 2. Osborn, J. A.; Jardine, F. H.; Young, J. F.; Wilkinson, G. *Journal of the Chemical Society A: Inorganic, Physical, Theoretical* **1966**, (12), 1711-32.
- 3. Trost, B. M.; Fleming, I.; Editors, Comprehensive Organic Synthesis: Selectivity, Strategy and Efficiency in Modern Organic Chemistry. 1992; Vol. 8, p 443-469.
- 4. Sinfelt, J. H. Accounts of Chemical Research 1987, 20, (4), 134-9.
- 5. Yu, Z.; Liao, S.; Xu, Y.; Yang, B.; Yu, D. Journal of Molecular Catalysis A: Chemical 1997, 120, (1-3), 247-255.
- 6. Richard, D.; Couves, J. W.; Thomas, J. M. Faraday Discussions 1992, 92, (Chem. Phys. Small Met. Part.), 109-19.
- 7. Pal, S.; Tak, Y. K.; Song, J. M. Applied and Environmental Microbiology **2007**, 73, (6), 1712-1720.
- 8. Bae, T.-H.; Tak, T.-M. Journal of Membrane Science 2005, 249, (1-2), 1-8.
- 9. Kim, S. H.; Kwak, S.-Y.; Sohn, B.-H.; Park, T. H. *Journal of Membrane Science* **2003**, 211, (1), 157-165.
- 10. Kwak, S.-Y.; Kim, S. H.; Kim, S. S. Environmental Science and Technology **2001**, 35, (11), 2388-2394.
- 11. Li, Q.; Chen, S.-L.; Jiang, W.-C. *Journal of Applied Polymer Science* **2007**, 103, (1), 412-416.
- 12. Ghule, K.; Ghule, A. V.; Chen, B.-J.; Ling, Y.-C. Green Chemistry 2006, 8, (12), 1034-1041.

13. Kim, Y. H.; Lee, D. K.; Cha, H. G.; Kim, C. W.; Kang, Y. C.; Kang, Y. S. *Journal of Physical Chemistry B* **2006**, 110, (49), 24923-24928.

